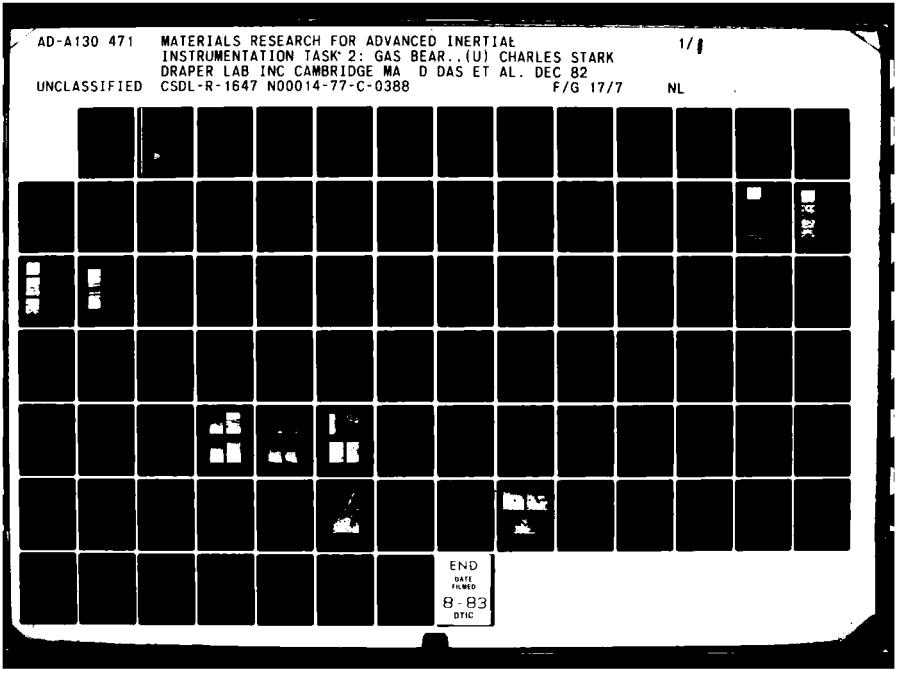
AD-A130 471 MATERIALS RESEARCH FOR ADVANCED INERTIAL INSTRUMENTATION TASK 2: GAS BEAR..(U) CHARLES STARK DRAPER LAB INC CAMBRIDGE MA D DAS ET AL. DEC 82
1/1
UNCLASSIFIED CSDL-R-1647 N00014-77-C-0388 F/G 17/7 NL
END
DATE FILMED
8-83
DTIC

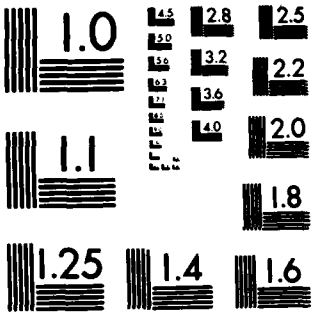

MICROCOPY RESOLUTION TEST CHART
NATIONAL BUREAU OF STANDARDS-1963-A

CSDL-R-1647

MATERIALS RESEARCH FOR ADVANCED INERTIAL INSTRUMENTATION

TASK 2: GAS BEARING MATERIAL DEVELOPMENT

DECEMBER 1982

TECHNICAL REPORT NO. 5
FOR THE PERIOD
1 OCTOBER 1981-30 SEPTEMBER 1982

BY

D. DAS and K. KUMAR

Prepared for the Office of Naval Research, Department of the Navy, under contract N000014-77-C-0388

The Charles Stark Draper Laboratory, Inc.
Cambridge, Massachusetts 02139

UNCLASSIFIED

SECURITY CLASSIFICATION OF THIS PAGE (When Data Entered)

REPORT DOCUMENTATION PAGE		READ INSTRUCTIONS BEFORE COMPLETING FORM
1. REPORT NUMBER CSDL-R-1647	2. GOVT ACCESSION NO. AD-A130 471	3. RECIPIENT'S CATALOG NUMBER
4. TITLE (and Subtitle) MATERIALS RESEARCH FOR ADVANCED INERTIAL INSTRUMENTATION; TASK 2: GAS BEARING MATERIAL DEVELOPMENT		5. TYPE OF REPORT & PERIOD COVERED Research Report 10/1/81 - 9/30/82 6. PERFORMING ORG. REPORT NUMBER CSDL-R-1647
7. AUTHOR(s) D. Das and K. Kumar		8. CONTRACT OR GRANT NUMBER(s) N00014-77-C-0388
9. PERFORMING ORGANIZATION NAME AND ADDRESS The Charles Stark Draper Laboratory, Inc. 555 Technology Square Cambridge, MA 02139		10. PROGRAM ELEMENT, PROJECT, TASK AREA & WORK UNIT NUMBERS
11. CONTROLLING OFFICE NAME AND ADDRESS Office of Naval Research Department of the Navy 800 N. Quincy St., Arlington, Virginia 20217		12. REPORT DATE December 1982 13. NUMBER OF PAGES 90
14. MONITORING AGENCY NAME & ADDRESS (if different from Controlling Office) Office of Naval Research Materials Division Arlington, Virginia 22217		15. SECURITY CLASS. (of this report) Unclassified 15a. DECLASSIFICATION/DOWNGRADING SCHEDULE

16. DISTRIBUTION STATEMENT (of this Report)

Approved for public release; distribution unlimited.

17. DISTRIBUTION STATEMENT (of the abstract entered in Block 20, if different from Report)

18. SUPPLEMENTARY NOTES

19. KEY WORDS (Continue on reverse side if necessary and identify by block number)

Beryllium	Boron	Beryllium-Ceramic Composite
Ion Implantation	Reactive Diffusion	Hot Isostatic Pressing (HIP)
CVD	Metal Matrix Composite	

20. ABSTRACT (Continue on reverse side if necessary and identify by block number)

Chemical vapor deposition (CVD) studies were continued with formation of additional boron coatings on beryllium. Problems encountered earlier with respect to coating thickness non-uniformity were corrected by installing a feed-through to the CVD chamber which permitted rotation of the samples during deposition. Questions pertaining to variability in coating quality, which was found to depend upon the particular gas cylinder selected for the diborane gas used during CVD, were successfully addressed through

DD FORM 1 JAN 73 1473 EDITION OF 1 NOV 65 IS OBSOLETE

UNCLASSIFIED

SECURITY CLASSIFICATION OF THIS PAGE (When Data Entered)

control of diborane gas concentration (by diluting it with Argon gas) and selection of an appropriate substrate temperature for deposition. Friction and wear tests performed on these recently formed coatings showed excellent wear resistance with very low friction coefficient values of the surfaces versus a diamond stylus serving as a pin. The performance against a sapphire pin, however, was quite poor with high measured values of the friction coefficient in agreement with observations reported earlier. These experiments indicated that the deposition temperature was not particularly critical in determining coating quality. Additional activities included Auger Electron Spectroscopy (AES) characterization of the surfaces that were tested for wear, and initiation of procedures for fabricating parts for evaluation after assembling into an actual gyro gas bearing configuration.

Work in the area of boron-implanted beryllium surfaces has concentrated on examination of the friction and wear behavior of graded boron implants with intended peak surface concentrations of 10, 20, and 30 atom percent boron. Polished beryllium surfaces were implanted and characterized for depth composition profiles using the AES technique. The data indicated that the "actual" boron concentrations were somewhat higher than the "intended" values and that the graded profiles were successfully obtained in most instances. Evaluation of wear and metallographic data with work reported earlier on graded and flat profile 40 boron atom percent "intended" peak concentration samples showed that no simple dependence of wear (and friction) performance on the peak intended boron concentration existed for the many samples that were examined. The overall results from this effort have been quite encouraging. Beryllium gas-bearing thrust plates implanted with the flat profile 40 atom percent boron concentration, which our results show to be superior to all of the other samples examined so far, are indicated to have strong potential for actual application.

Be-TiB_2 composite material evaluation for gas bearings continued with work on composites containing different sizes of TiB_2 particles. Lapping procedures, investigated and reported earlier, were further refined for producing nearly damage-free microstructures. Friction and wear tests showed that the best performance was observed versus a diamond stylus serving as the pin whereas poor results were obtained when sapphire and (a similarly) fabricated) composite pin were used. These experiments, and subsequent wear track examination using a scanning electron microscope, showed little relative difference between the wear performance of the +30μm and the -10μm TiB_2-containing composites. Studies were also performed on ultrasonic cleaning procedures for these composites with the aim of determining their effect on material integrity. These studies indicated that the effect of ultrasonic processes on material integrity was perhaps not too severe and that properly consolidated parts could be thoroughly cleaned using ultrasonic baths. Experiments were also initiated at fabricating near-net shape gas bearing parts, composed essentially of beryllium with a thin surface consisting of the composite composition at the rubbing surfaces of the gas bearing parts.

CSDL-R-1647

MATERIALS RESEARCH FOR ADVANCED INERTIAL INSTRUMENTATION

TASK 2: GAS BEARING MATERIAL DEVELOPMENT

DECEMBER 1982

TECHNICAL REPORT NO. 5

FOR THE PERIOD

1 October 1981 - 30 September 1982

D. Das, K. Kumar

Prepared for the Office of Naval Research,
Department of the Navy, under Contract N00014-77-C-0388.

Approved:

M.S. Sapuppo, Head
Component Development Department

The Charles Stark Draper Laboratory, Inc.
Cambridge, Massachusetts 02139

ACKNOWLEDGEMENT

This report was prepared by The Charles Stark Draper Laboratory, Inc. under Contract N00014-77-C-0388 with the Office of Naval Research of the Department of the Navy.

Publication of this report does not constitute approval by the U.S. Navy of the findings or conclusions contained herein. It is published for the exchange and stimulation of ideas.

TABLE OF CONTENTS

TABLE OF CONTENTS (continued)

LIST OF FIGURES

LIST OF FIGURES (continued)

LIST OF TABLES

SECTION 1

INTRODUCTION

In the construction of inertial instruments, the purely structural requirements, with respect to strength, stiffness, and creep, can be met for most purposes through the use of instrument-grade beryllium. The mating surfaces of the gas bearings of these instruments demand higher hardness and greater wear resistance than beryllium offers. A variety of combinations of materials and processes consisting of solid ceramics and arc-plasma sprayed or sputter-deposited ceramics on beryllium surfaces have been used. None of these was found to be completely satisfactory either because of thermal expansion and conductivity mismatch or because of poor adhesion and existence of porosity.

The material of choice in the fabrication of structural members for state-of-the-art inertial instruments is beryllium, primarily because of properties such as high values of stiffness, thermal conductivity, and the strength-to-density ratio that it possesses. Unfortunately, gas bearings used in such instruments require substantially greater hardness and wear resistance at the mating surfaces than beryllium offers.

Gas bearings initially built at The Charles Stark Draper Laboratory, Inc. (CSDL) involved fabricating entire bearings out of solid pieces of ceramic. These ceramics were typically produced by sintering and hot pressing techniques. Difficulties were encountered in machining these materials, making the process expensive and time consuming. An additional disadvantage in the use of ceramics for this purpose was the physical incompatibility of the resultant gas bearings with the other structural members of the gyro. Differences in thermal expansion characteristics and low values of thermal conductivity of these materials result in undesirable strains and temperature variations in the assembly. This leads to a variety of instrument instabilities

that adversely affect the accuracy and reliability of the several inertial components. The high cost in money and time, in addition to the problems stemming from low values of thermal expansion and thermal conductivity for ceramics, caused this option to be discarded.

The subsequent rationale developed to resolve the discrepancies envisioned the use of two different materials, since no single material was known to meet all demands. One material (beryllium) was to form the structural member and satisfy bulk property requirements. The other was to be deposited as a coating to yield a low-friction, wear-resistant surface for the gas bearing. Operational and processing problems have, nevertheless, persisted even with the approaches that resulted from this rationale and a better materials system is needed. The present task addresses this latter requirement through research efforts on new materials and processes for gyroscope gas bearings.

1.1 Property Requirements

The property requirements of the coatings formed on gas bearing surfaces are summarized as follows:

(1) High resistance to wear from sliding, erosion, and impact, for extended bearing life and stable performance

(2) Low coefficient of friction for minimum starting torque

(3) Zero surface porosity, for maximum gas bearing stiffness and minimum contamination entrapment

These property requirements necessitate the selection of ceramic-type compositions for coating fabrication. Two methods of applying such coatings that have received attention in this area are plasma-spraying and sputtering, the former enjoying the wider use in production. With plasma spraying it is easy to apply coatings which are several thousandths of an inch thick, while the thicknesses of sputtered films are generally less than that by about two orders of magnitude. Examples

of the use of these processes are the plamsa-sprayed chromium oxide and aluminum oxide coatings now in use in several instrument designs and the sputter-deposited tungsten carbide and titanium carbide coatings that have been subjects of some past development activity.

1.2 Limitations of Present Technologies

The one feature common to both sprayed and sputtered coatings is the difference in physical properties between the coating and the substrate. While this may be somewhat tolerable in thin films produced by sputtering, thicker films made by spraying are susceptible to failure from the imperfect match of expansion coefficients at the coating-substrate interface. To reduce stresses that result from differences in expansion coefficients, spraying is generally conducted at lower spray temperatures. However, this adversely affects interparticle cohesive strength, which results in pull-outs during polishing and lapping operations, and generation of wear debris in active service. The clearance between the mating parts of a gas bearing is only about 50 microinches so that even the mildest form of wear (mildest by conventional standards) can prove to be catastrophic in gas bearing applications.

A more severe problem that has been found in sprayed deposits is the presence of interconnecting porous structures in the coating. The effect of this interconnected porosity is to provide a shunt path for gas flow such that the hydrodynamic pressure rise is attenuated from that attainable with a nonporous coating.[1]* This, in turn, causes a lower load capacity and stiffness for the gas bearing. In addition to this most severe effect, the porosity at the surface also results in effectively increasing the bearing gap beyond the physical (design) clearance.

The adhesion of the coating to the substrate is an important consideration in wear performance. The forces that give rise to adhesion in films made from both these processes can be both mechanical

* Superscript numerals refer to sources in the List of References.

and chemical in nature. The adhesion observed for deposits fabricated using the arc-plasma technology is generally found to be influenced by mechanical interlocking of the film on the external features of a substrate.

In chemically compatible coating-substrate systems, the adhesion strength can be increased by depositing films at elevated temperatures. Elevated temperature deposition is preferable to post-deposition heat treatment since ceramic materials generally behave well under mild compressive loading.

Poor adhesion has been the biggest problem with sputtered ceramic coatings formed on beryllium substrates.[2] Sputter-deposited films have also shown large deviations from stoichiometric composition and the presence of undesirable microstructures.

1.3 Direction of the Present Work

The broad objective which underlies all aspects of the present effort is to establish a hard, pore-free, wear resistant surface which is integral with the beryllium structural members, thus eliminating the adhesion problems that have been encountered in the past. In the case-hardening subtask, this is approached by treating a beryllium surface with boron at elevated temperatures, with which it forms hard compounds. Boron enrichment of the surface, in one process, is accomplished by reactive diffusion of a freshly formed film of boron with the underlying beryllium. In another part of the work, boron ions are forced by an electrical potential to penetrate into the beryllium surface by ion implantation, a process which is relatively immune to native oxide barriers, solubilities, and diffusion coefficients.

In a second subtask the desired hardening and wear resistance are imparted by particles of a hard ceramic phase dispersed within the beryllium matrix. Such a metal-matrix composite is produced using powder metallurgy methods.

SECTION 2

BERYLLIUM-BORON REACTIVE DIFFUSION BY CVD

2.1 Background

The primary goal of this subtask of the gas-bearing materials program was to produce a wear-resistant, low-friction, hard surface on beryllium by reactive diffusion with boron. A secondary objective of the program was to study the relevant diffusion kinetics in the Be-B system, in order to be able to exercise control on the structural and dimensional characteristics of the coating.

The binary alloy system Be-B contains a number of intermetallic compounds, of which the compounds BeB_6 and BeB_2 are reported to have hardness values of 2600 and 3200 KHN, respectively.[3,4,5] Boron also has a hardness value of nearly 3000 KHN. Therefore, reactive diffusion of boron is an attractive means of producing a metallurgically bonded hard coating on the beryllium surface.

2.2 Progress Prior to This Report

Early attempts of bonding boron, either in powder or solid form, by hot pressing on the beryllium surface, were unsuccessful. A well-bonded interface between the two elements, however, was formed when solid boron was hot isostatically pressed (HIP) with cold compacted beryllium powder surrounding it. It was possible to obtain Be-B diffusion couples out of these HIP configurations by careful machining. Diffusion heat treatments, however, produced unexpected failures as a result of the beryllium physically separating from the diffusion interface. The intended studies of diffusion kinetics using conventional diffusion couples therefore had to be abandoned.

In a parallel effort it was determined that boron could be chemically vapor deposited (CVD) from a gaseous boron source on a heated beryllium surface, to produce adherent thin film coatings with high

hardness values. Of the two gaseous CVD systems, (1) chemical reaction of BCl_3 with H_2[6] and (2) thermal decomposition of diborane (B_2H_6),[7] the first one was found to be satisfactory at temperatures of 900°C and higher. At lower temperatures of operation, which are more desirable for beryllium substrates, B_2H_6 turned out to be the superior system. Initial experiments were performed inside a 1-1/4-inch-diameter quartz tube evacuable to 10 millitorr pressure prior to the introduction of the CVD gas. The samples were heated by RF induction with a coil wrapped around the quartz tube where the sample was located. At CVD temperatures of 850° to 900°C, coatings with a maximum thickness of 1 μm were formed with rusty pink color and maximum microhardness values of about 1200 KHN. As much as 5-μm-thick steel gray color coatings with microhardness values exceeding 2000 KHN were subsequently formed at CVD temperatures of 700° to 800°C. At this point it became apparent that thicker coatings of higher microhardness values would require a cleaner CVD system.

A new CVD system was built, consisting of a stainless steel bell jar equipped with high vacuum pumping systems and all stainless steel plumbing. The system was capable of being baked out and achieving a high vacuum of about 10^{-7} torr. A 20-kw RF generator was acquired for furnishing the induction heating power to the coil located inside the bell jar, which permitted increasing the sample size from 1/2-inch-diameter discs to much larger sample sizes by the use of larger coils. Present capability is therefore adequate for producing CVD coating on actual gas bearing components. Initial experiments in this new system were carried out on 1/2-inch-diameter samples using a 3/4-inch inner diameter (ID) RF coil. The CVD procedure involved evacuating and baking out of the system at a low temperature of 100°C, following which the CVD was carried out using diborane gas (99.9% A and 0.1% B_2H_6) at atmospheric pressure. During the CVD run the bell jar was water-cooled to prevent evolution of undesirable gases from the CVD chamber walls. Well bonded coatings, as much as 10 μm thick with uniform coverage of the entire 1/2-inch-diameter surface, were obtained at 700° and 800°C.[8] Microhardness values exceeded 3000 KHN measured under a 25-gram indentation load. The low-temperature CVD samples prepared in the older CVD apparatus had hardness

values of approximately 1000 KHN at the 25-gram load, although at a 5- to 10-gram load the measured values were above 2000 KHN. The quality had therefore improved substantially.

Metallography, electron diffraction, and Auger analysis of these latest samples suggested that the CVD coatings consisted of an amorphous outer layer of boron with a layer of mixed beryllium borides at the interface. It appeared that post-CVD heat treatments were capable of yielding limited information on diffusion kinetics in the Be-B system. However, the same treatments were not likely to produce useful bearing surfaces with Be-B compounds, because of the mechanical damage to such surfaces as a result of these treatments. If BeB_6 or BeB_2 surfaces were to be produced at all, it appeared that it had to happen during the CVD process.

Scaling up from 1/2- to 3/4-inch-diameter samples, which was accomplished by using a 1-1/4-inch-diameter RF coil instead of the 1-inch diameter coil, presented no special problems, and indicated that actual gas bearing components could be produced in the present system. The 3/4-inch-diameter samples were used for wear and friction measurements, using pin-on-disc testing. For all these preliminary tests a 1/8-inch sapphire ball was used as the pin. Measured coefficients of friction were all about 0.4, which is rather high, although under the same conditions of measurement polished beryllium yielded a value of 0.8. The wear tracks were deep grooves, but the CVD coating appeared to be wear-resistant, as evidenced by smooth walls and no signs of plowing or pullouts.

The CVD film thicknesses were found to be nonuniform, the coating being heavier at the bottom parts with gradual decrease of thickness to the top. The nonuniformity was attributed to convection currents in the CVD gas around the hot beryllium sample during the deposition process.

2.3 Progress during the Reporting Period

The experimental investigations were performed in the following areas:

(1) Uniform film thickness

(2) CVD gas composition studies

(a) Wear and friction tests

(b) Auger analysis

(c) Fabrication of gas bearing parts

(d) Personnel safety evaluation

2.3.1 Uniform Film Thickness

In last year's annual report[8] the lack of uniformity of the CVD boron coatings on the beryllium surface was clearly demonstrated during the preliminary wear and friction testing of the samples. The disc-shaped samples were held stationary during the CVD in a vertical plane, perpendicular to the direction of gas flow. It was found that the CVD films were heavy at the bottom and thin at the top. The nonuniformity was believed to have been caused by the convection currents of the CVD gas around the hot beryllium disc. As a result of the nonuniformity, the grooves or wear tracks were from three to six times wider and two to four times deeper in the thin regions as compared to the thick areas. There was, therefore, a need to modify the operation to produce coatings of uniform thickness over the entire surface.

Since the bottom parts of the disc had the heaviest coatings and the thickness gradually decreased going towards the top, it appeared that the uniformity of the film thickness could be accomplished by rotating the disc about its axis during the deposition. A rotational fixture was procured commercially. The fixture provided a 1/4-inch

rotating stainless steel shaft on one end, which was located inside the CVD bell jar. The other end of the fixture had a similar shaft which remained outside the bell jar. The outside shaft was rotated by a low-r/min motor and the rotational motion was transmitted to the inside shaft through a bellows connection. The fixture was mounted on a stainless steel flange which was then connected to the bell jar on a matching flange using an O-ring seal. These mountings were so located that the inner shaft pointed to the axis of the RF coil inside the bell jar, with some lateral adjustments for centering the specimens. The beryllium disc was attached to the rotating shaft by extensions made from a machinable glass (Macor) and a further stainless steel threaded extension. The latter arrangement prevented excessive thermal conduction to the bellows. It was possible to locate the beryllium disc sample concentric with the RF coil and at the mid-plane between the two ends of the coil. A 10-r/min motor capable of producing 30-in-oz torque provided the desired rotation to the outer shaft of the fixture.

Since the installation of the rotational mechanism, a large number of beryllium disc samples have been CVD coated with boron. The coating thickness has been quite uniform and the operation of the fixture has presented no problems.

2.3.2 CVD Gas Composition Studies

The studies to be described in the following were performed because of a lack of reproducibility of the CVD gas mixture used until about October of 1981. The gas mixture of 99.9% Argon and 0.1% diborane (B_2H_6) was prepared by and purchased from the Matheson Co. Of the two standard 200-ft^3 gas cylinders purchased initially in late 1979, one gave excellent adherent boron coatings during CVD and the other produced nonadherent, sooty deposits. Two new cylinders with the same nominal gas composition were purchased from the same vendor after the first good one was expended. These new ones also produced sooty deposits under the same CVD gas-flow conditions of one liter per minute. It was also determined that when the gas flow from the original satisfactory cylinder was increased to higher flow rates, the deposits became sooty. The preceding facts led to

the conclusion that either the first gas mixture cylinder had less than the specified 0.1 percent diborane or else the other cylinders contained more than the specified amount. Therefore, if the gas from these new tanks was diluted with additional pure argon they should produce satisfactory CVD coatings. The dilution was accomplished by allowing the gases from an argon cylinder and the argon plus diborane cylinder to flow at desired rates through parallel lines and individual flow meters into a mixing chamber. The new gas composition thus created in the mixing chamber was then allowed to flow into the CVD chamber at the desired flow rate.

With the preceding arrangement, a CVD run was performed in the usual manner on a 3/4-inch-diameter beryllium disc using the following experimental conditions: rotating disc maintained at a temperature of 725°C, with a gas flow of 36 cm^3/min of A and DB plus 800 cm^3/min of pure argon for a period of three hours. Upon removal from the CVD chamber the sample surface was found to be shiny metallic gray, darker in appearance than the polished beryllium surface before the CVD. It should be remembered that this same tank of A and DB gas mixture had previously produced only nonadherent, sooty deposits. To confirm the new sample surface to be truly a CVD coating, instead of a tarnished beryllium surface, many different analytical procedures could be used. But a quick qualitative confirmation is a microhardness measurement of the surface. The measurement showed that the sample had the hardness values of about 1400 KHN at a 10-gram load and about 1800 KHN at a 5-gram load. Beryllium shows the hardness values of about 400 to 600 KHN under 5- to 10-gram indentation loads. The sample therefore had a coating formed during the CVD operation, which could be either boron or a compound of beryllium and boron. More detailed information about the exact chemical composition of the surface could be determined later by other analytical procedures. But for the time being we had successfully produced a hard coating by dilution of the diborane gas mixture. Also, it was evident that the coating was fairly uniform, as indicated by the hardness values of various different areas of the sample.

Having solved the mystery of reproducibility of the argon and diborane mixture, we proceeded to make a number of CVD runs, under conditions of varying (1) gas composition, (2) substrate temperature, and (3) length of deposition time. Table 1 shows the various runs performed and the quality of the CVD coating produced as indicated by visual examination.

Table 1. Quality of the CVD coating dependent on temperature, time, and gas composition.

Sample No.	Substrate Temp, °C	Deposition Time (hrs)	Gas Flow rate, cm^3/min		Coating Quality Remarks
			B_2H_6	A	
65	725	3	36	800	Adherent, metallic gray, shiny
66	725	2	72	800	Nonadherent, sooty
67	725	3	36	800	Repeat of No. 65. Results same as No. 65.
68	725	3	54	800	Hard, adherent, gray
69	725	3	45	800	Shiny gray
70	725	1.5	63	800	Pink, adherent
71	725	1.7	63	800	3 additional hours at room temp. in argon. Shiny, gold.
72	825	2	72	800	Adherent, shiny blue
73	825	1	72	800	Adherent, shiny silvery
74	825	0.5	72	800	Adherent, shiny blue-gray
75	825	4	72	800	Dull gray, adherent

At the CVD temperature of 725°C, good and adherent coatings could be formed with the gas flow rate of as much as 63 cm^3/min for the argon and diborane mixture. At 72 cm^3/min gas flow the deposit became sooty and nonadherent. A few more experiments (sample numbers 76, 77, and 78, not

shown in Table 1) underwent a CVD run at the gas flow rates of 110, 150, and 300 cm^3/min, all of which produced nonadherent and sooty deposits. Sample numbers 72, 73, 74, and 75 had CVD runs at 825°C at a gas flow rate of 72 cm^3/min for time periods of one-half hour to four hours. In each of these cases the depositions resulted in sound adherent films. Obviously, higher temperatures would permit higher gas flow rates because of higher diffusion rates. Any further exploration of time, temperature, and gas flow rates was postponed at this stage in order to perform some important investigations, such as wear and friction studies and Auger analysis, on a large number of good samples that had already been produced to ascertain if we had produced some desirable candidates for gas bearing application.

2.3.2.1 Wear and Friction Tests

In the last report,[8] preliminary wear tests on CVD samples were described. Briefly, the method used was the pin-on-disc type, where the pin was stationary and the sample disc was rotated. The pin used was a 1/8-inch-diameter sapphire ball. The sample disc was rotated at 200 r/min. Calculated friction coefficient was approximately 0.4. Although there was no evidence of plowing or pull-outs, the groove widths and depths were quite high. It was suspected that the rotational speed of 200 r/min caused excessive vibration in the apparatus, giving undependable test results. Since then, more tests were performed on the same CVD samples using a speed of 100 r/min. The grooves were shallower and less wide and the friction coefficients were about the same.

It was decided to perform wear tests on the present samples using a sample rotational speed of 100 r/min. All the samples shown in Table 1 were tested at 100 r/min, using a 1/8-inch sapphire ball as the stationary pin with loads of 20, 25, and 30 grams. All of the runs were of 10-minute duration. Prior to the wear testing, the sample surfaces were given a polish which removed about 2 μm of the coating thickness. There was still about 2 μm of the film left on the beryllium surface, as was seen later during the depth profile Auger analysis of the samples. Friction coefficients calculated from the wear test data were found to be consistently quite high, although the wear did not appear to be too

large. Further wear tests on these samples were performed using a diamond ball as the pin. The load used was 23 grams and the samples were rotated at 100 r/min. The calculated friction coefficients for each of the test runs are shown in Table 2.

Table 2. Calculated friction coefficients during wear testing of CVD samples.

Sample Number	Friction coefficient - sapphire ball at loads of:			Friction coefficient using diamond pin at 23 gm
	20 gm	25 gm	30 gm	
65	0.36	0.28	0.50	0.16
67	0.41	0.35	0.23	0.11
68	0.68	0.62	0.43	0.06
69	0.79	0.75	0.83	0.07
70	1.23	1.20	1.05	0.07
71	0.87	1.06	0.97	0.07
72	0.42	0.33	0.33	0.32
73	0.99	0.75	0.92	0.13
74	1.00	1.21	0.82	0.13
75	1.25	1.49	1.50	0.18

A few facts can be gleaned from the friction coefficient data shown in Table 2. The friction coefficient is much higher with the sapphire pin than with the diamond pin, which appears to be the most important fact. The temperature of deposition does not appear to have great significance. Larger gas flow rates during deposition appear to have produced higher friction coefficients against the sapphire pin, although the reverse is true for the diamond pin.

The wear tracks of all the samples were photographed in the Nomarski mode and were also analysed by profilometry using a Dektak profilometer. The results of these examinations are shown in Figures 1 through 4 for a few selected samples, such as samples 65, 69, 74, and 75. The wear track grooves caused by the sapphire pin are quite distinct and measurable. However, the wear tracks due to the diamond pins, although visible in

Nomarski pictures, are not that easily distinguished in the Dektak traces from the surrounding background. The wear of the surfaces by the diamond pin was therefore negligible. The sapphire pin, however, showed considerable wear of the surfaces in all cases. Distinct grooves were formed in some cases such as sample numbers 65 and 75, shown in Figures 1 and 4. In other cases the wear tracks were actually build-ups rather than grooves. Sample Nos. 69 and 74, shown in Figures 2 and 3, are examples of build-ups. It is presumed that the build-ups are the results of erosion and smearing of the sapphire pins.

For each Nomarski picture a corresponding Dektak trace is shown directly below the photograph. Because of the large depth of focus of the microscope in the Nomarski mode the grooves appear to be in focus. The photographs were taken at a 205X magnification, which corresponds well with the 200X magnification (2-cm chart paper for 0.01-cm pin travel on the sample) in the horizontal direction of the Dektak trace. The magnification of the Dektak trace in the vertical direction, showing the depth of the wear track groove, is 50,000X (1 cm on chart equals 2000 Å of groove depth).

2.3.2.2 Auger Analysis

As explained in previous reports of this program, the most promising technique for analysis of thin films consisting of boron and/or beryllium is the Auger analytical procedure. Therefore, it was decided to carry out Auger analysis on the present samples. The procedure used was to continuously remove material away from the coated surface by sputtering with argon ions. While the material was being removed, chemical composition of the exposed surface was being determined by Auger technique. The composition data thus obtained were plotted against sputtering time. The depth of the sputtered holes was measured after the Auger analysis and the rate of sputtering was determined. The measured value of the sputtering rate for the present procedure was found to be 0.041 μm/minute. The depth profile data are presented for sample numbers 65 through 74 in Figures 5 through 13. The depth data is left as sputtering time, which can be converted to μm by multiplying the number of minutes by 0.041.

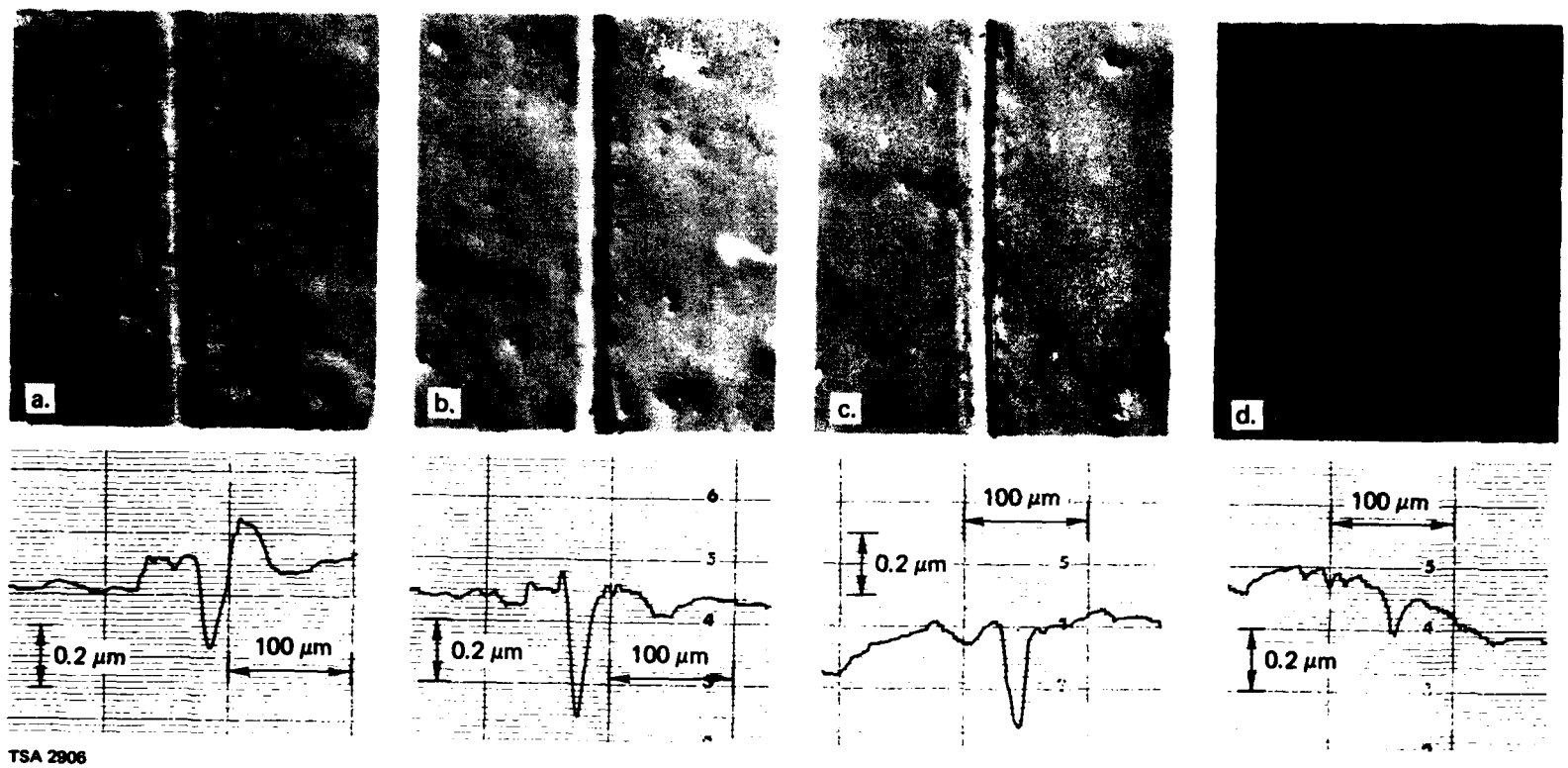

Figure 1. Wear tracks on sample No. 65 shown by Nomarski photographs and Dektak traces. A, B, and C with 30, 25 and 20 gm load respectively on saphire pin. D with diamond pin with 23 gm load.

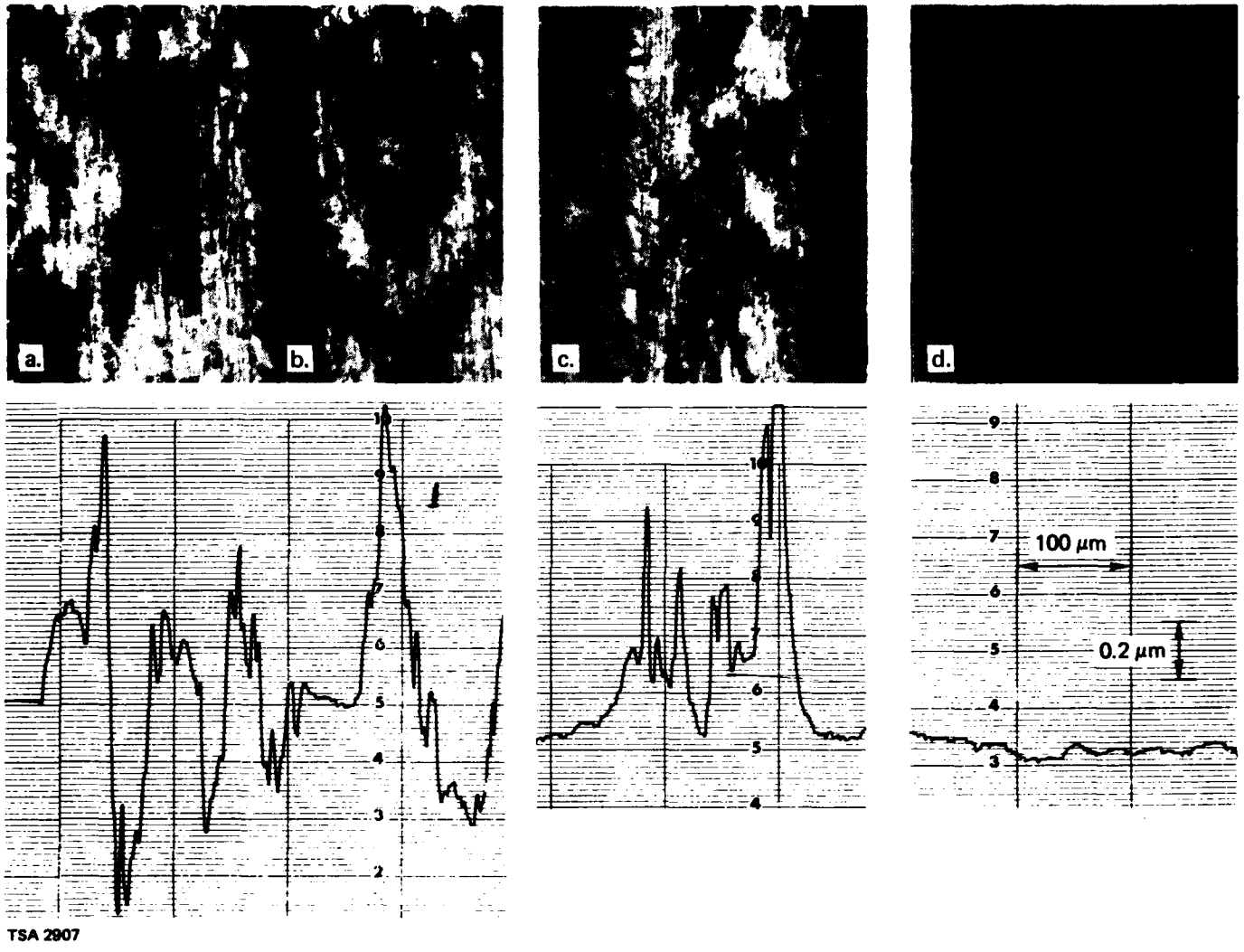

Figure 2. Wear tracks on sample No. 69. A, B, C, - saphire pin with 30, 25 and 20 gm loads. D - diamond pin with 23 gm load.

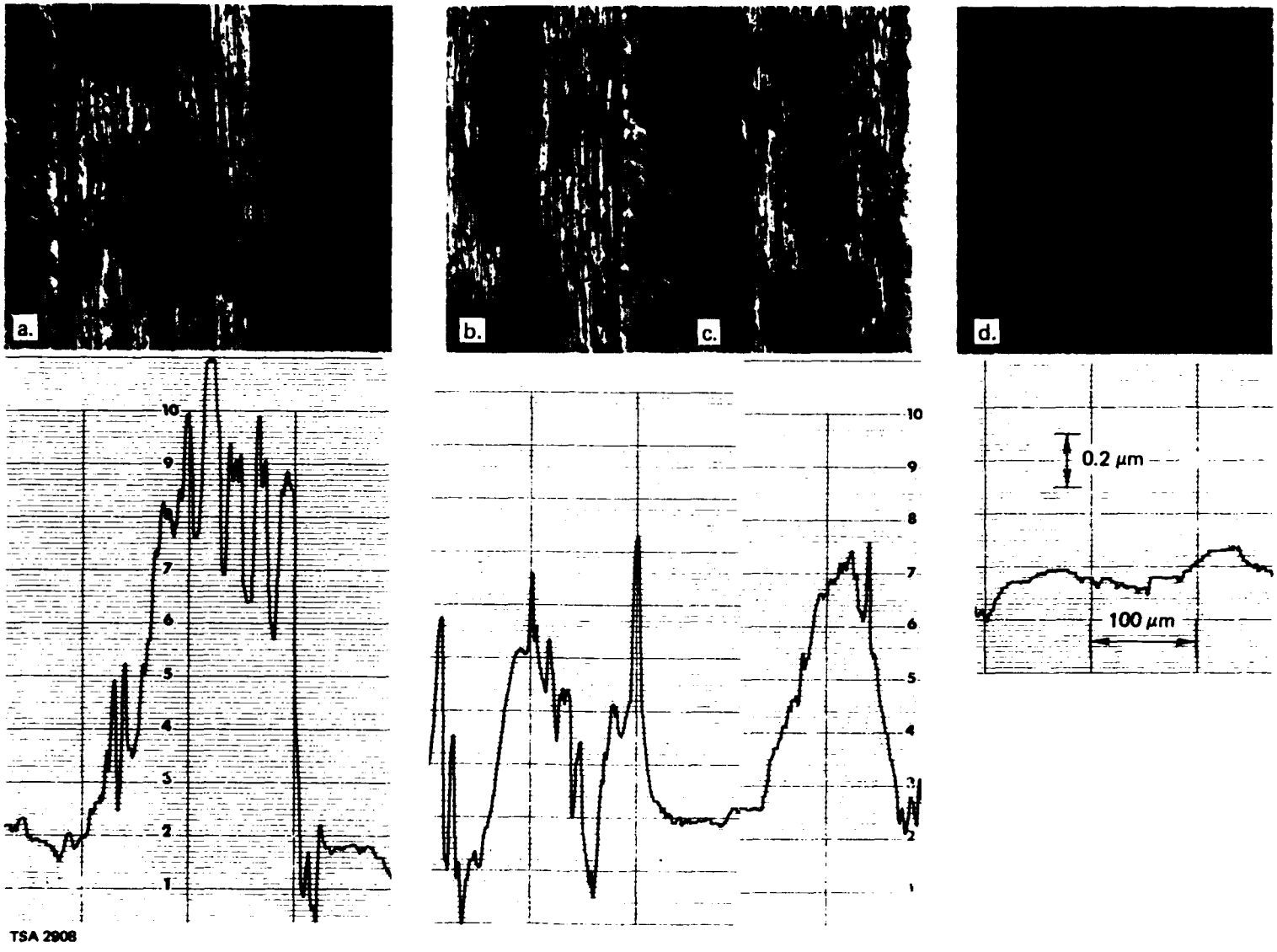

Figure 3. Wear tracks on sample No. 74. A, B, C -saphire pin with 30, 25 and 20 gm loads. D- diamond pin with 23 gm load.

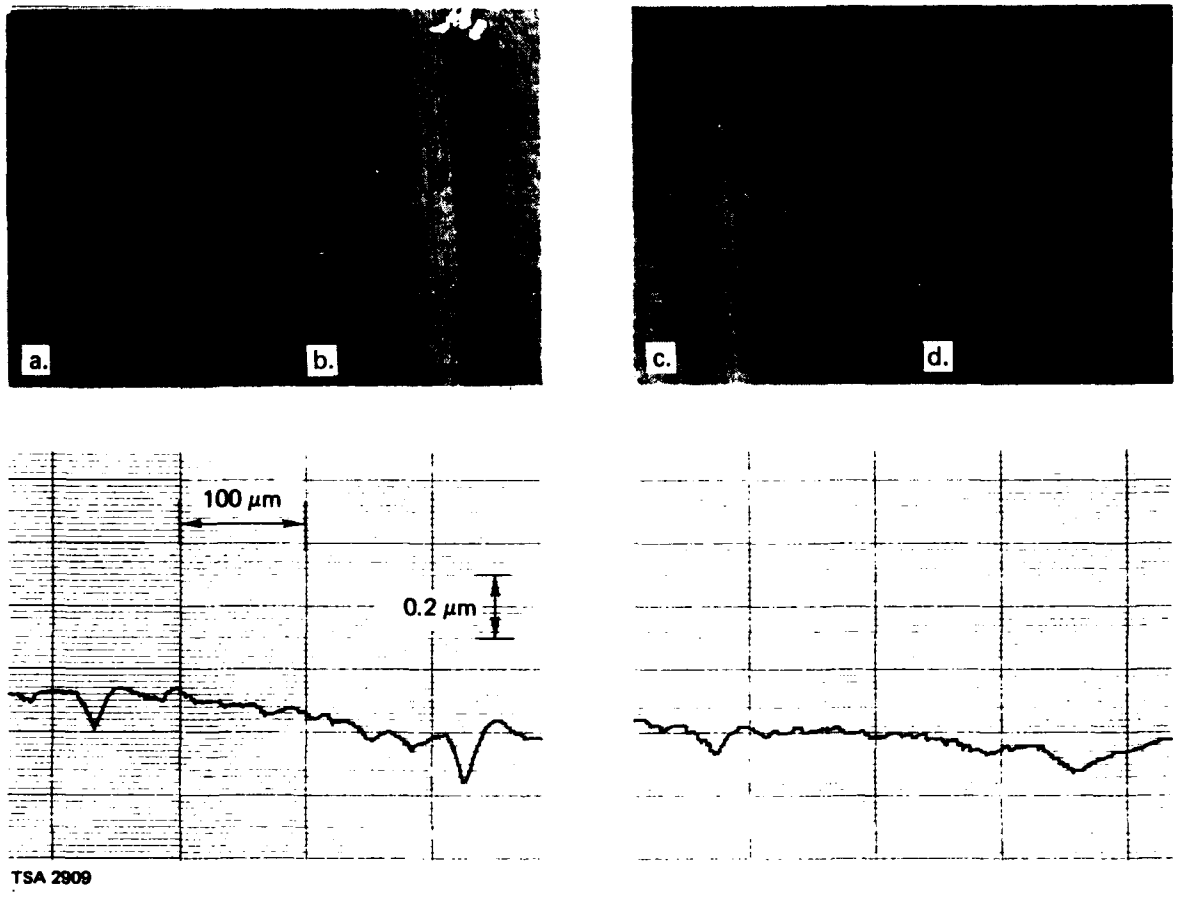

Figure 4. Wear tracks on smaple No.75. A, B, C - saphire pin with loads of 30, 25 and 20 gm loads. D- diamond pin with 23 gm. load.

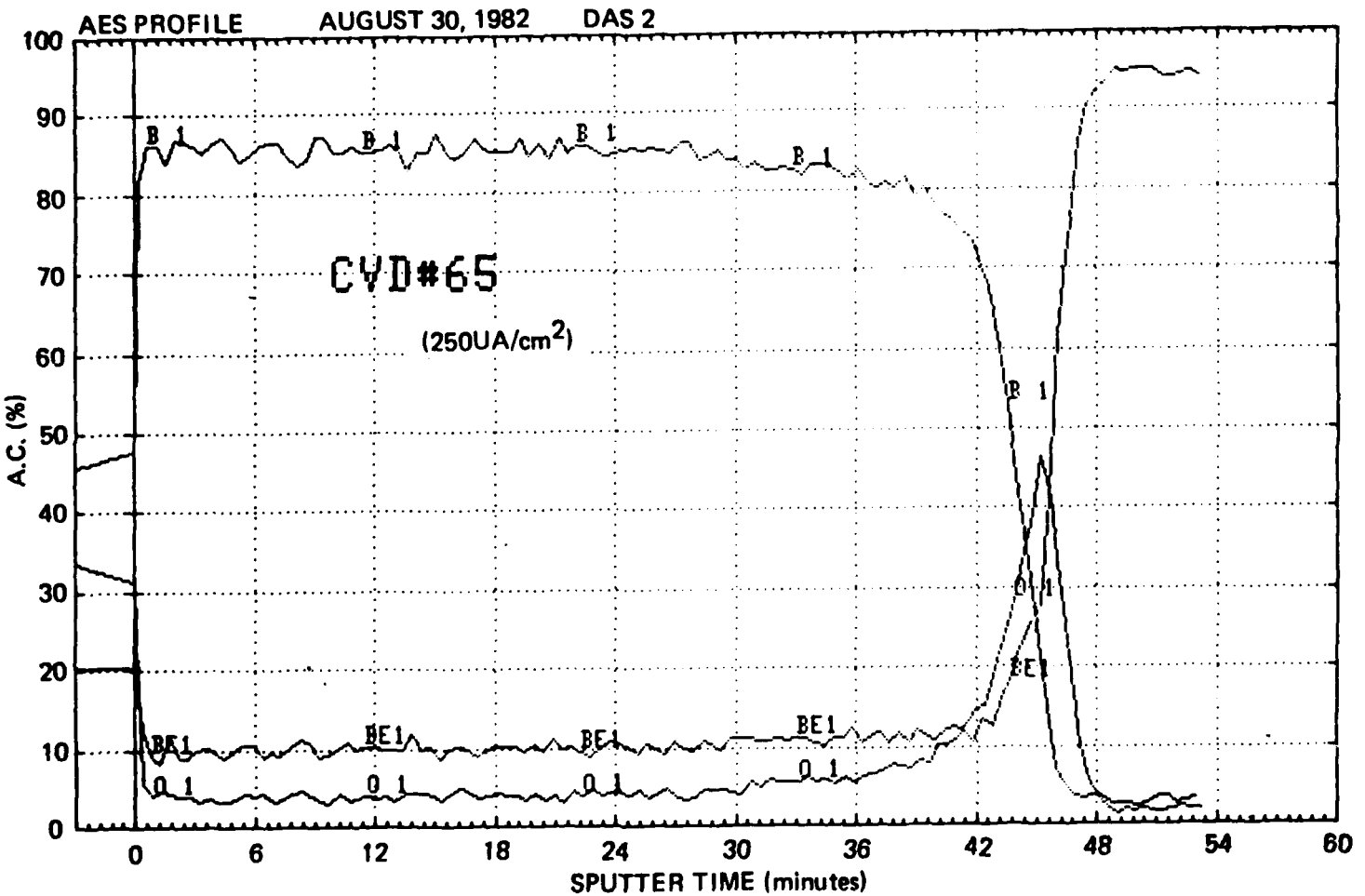

Figure 5. Auger depth profile of sample No. 65. Sputtering rate = 0.041 μm/min.

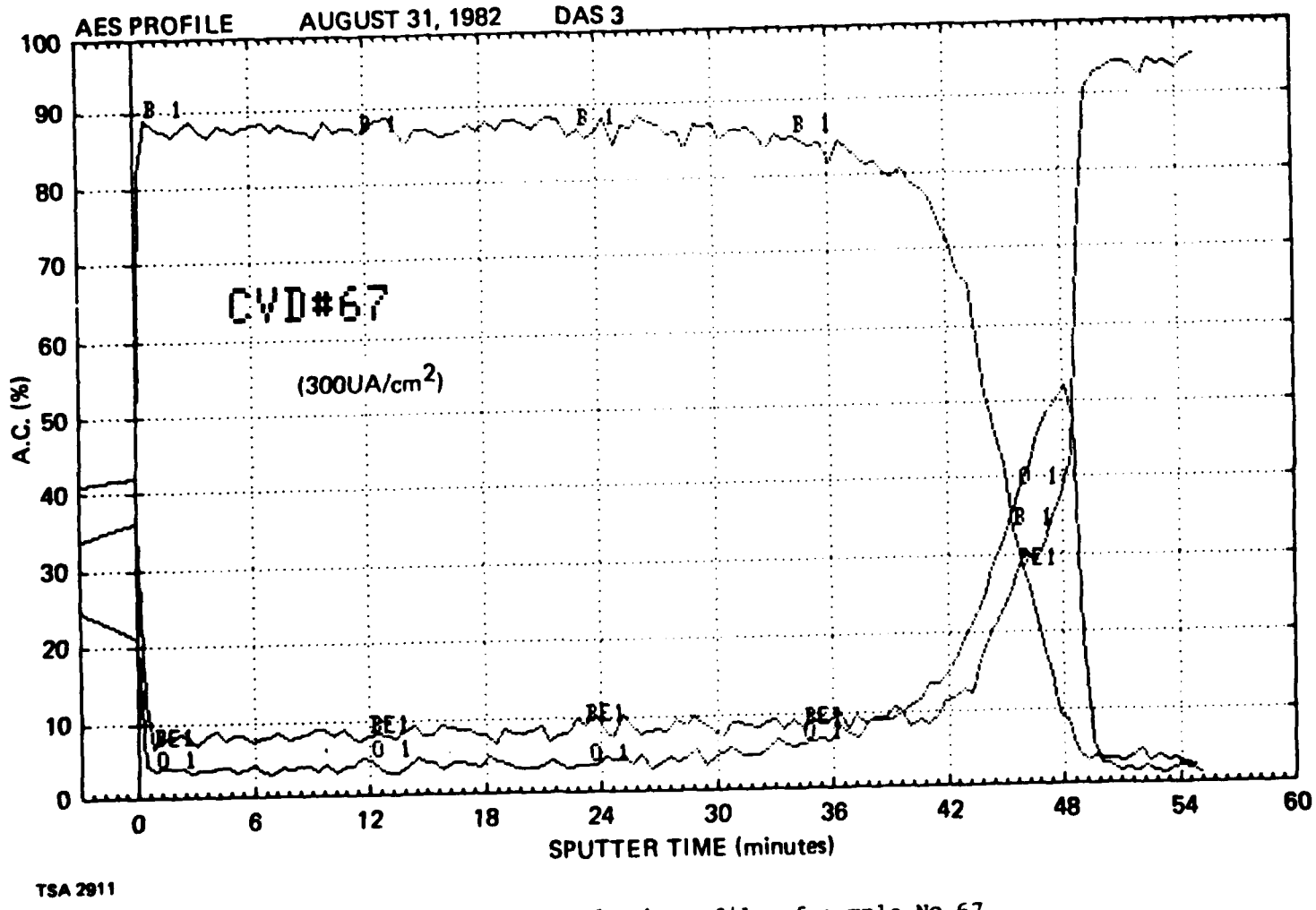

Figure 6. Auger depth profile of sample No.67

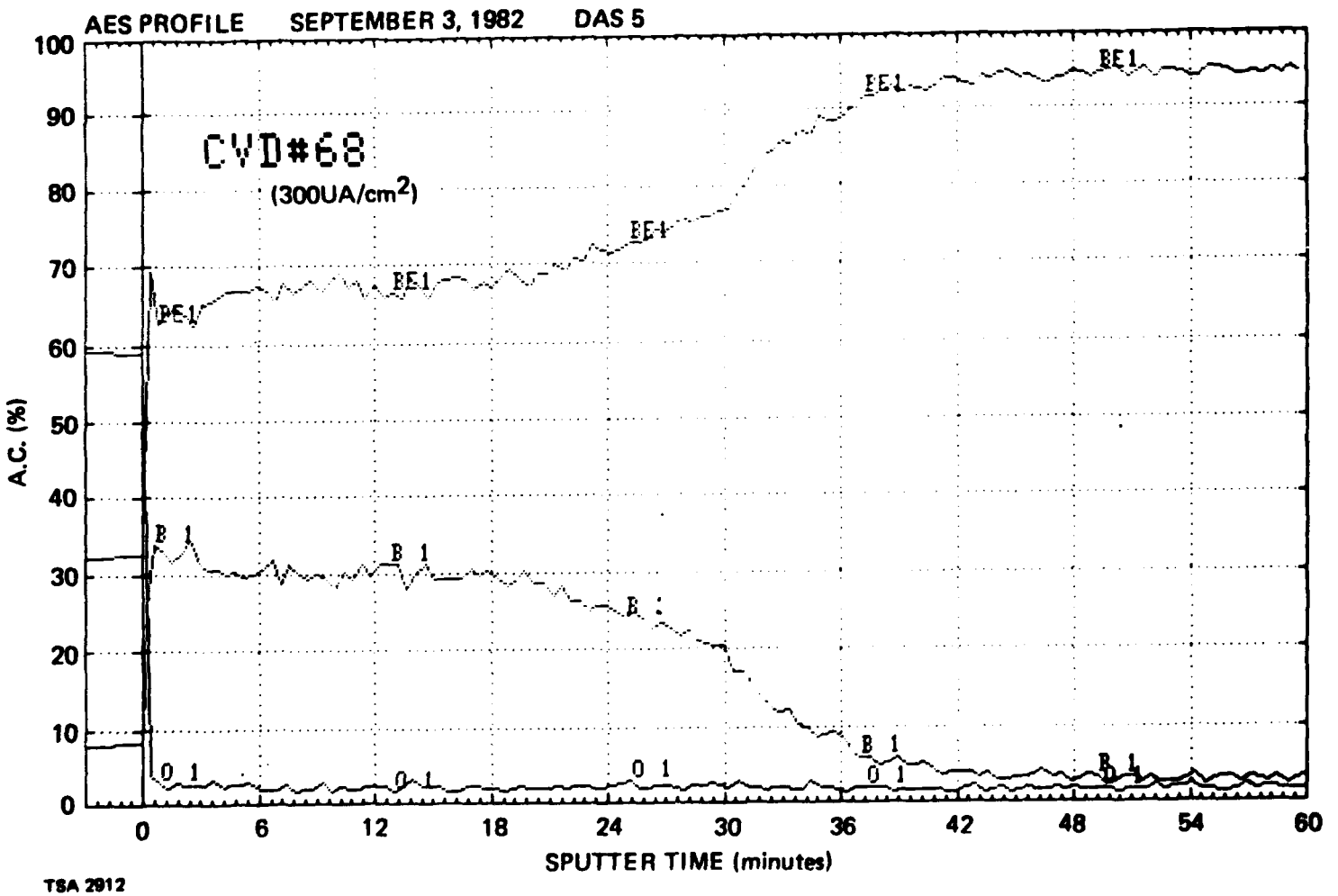

Figure 7. Auger depth profile of sample No.68

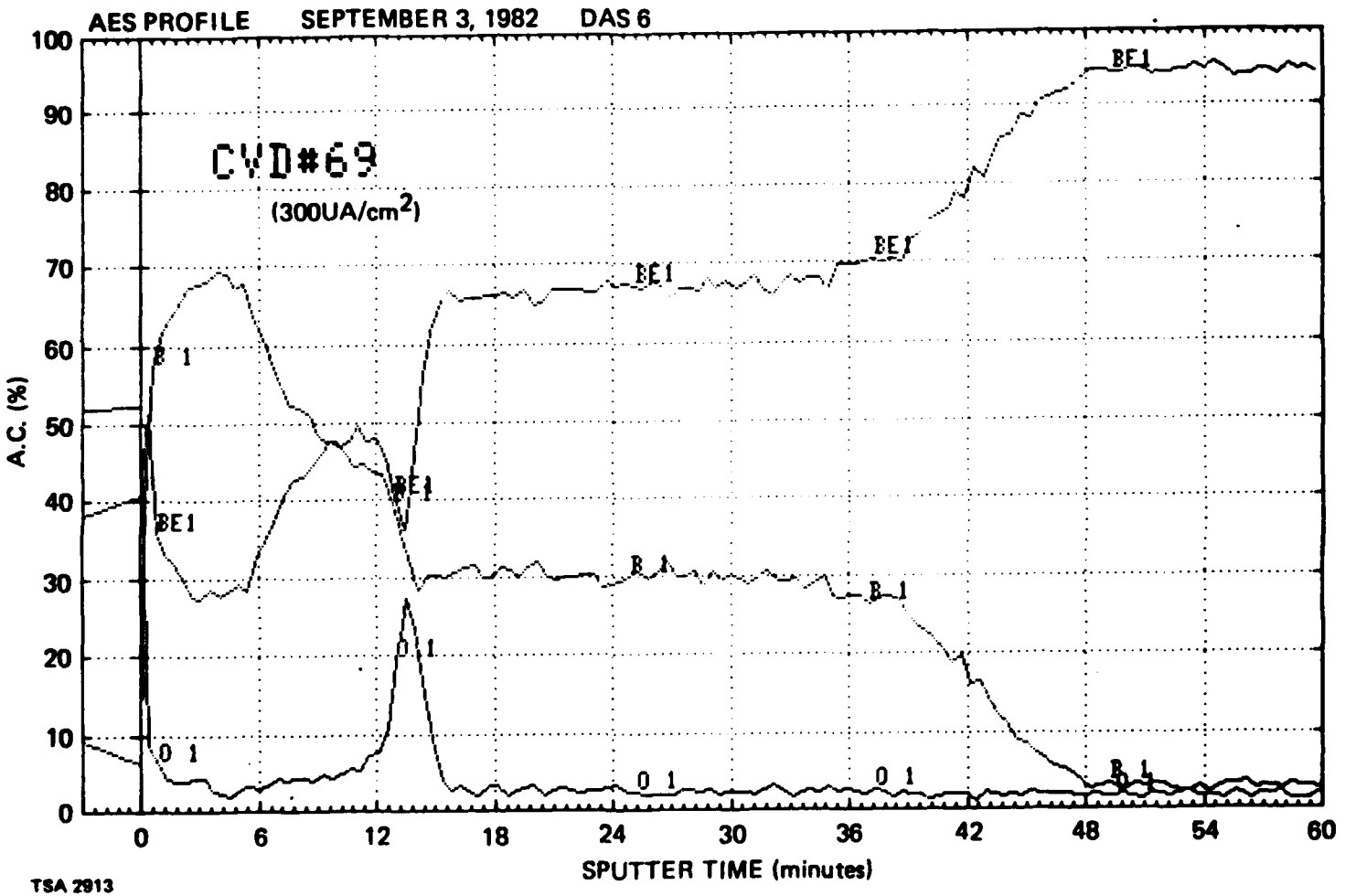

Figure 8. Auger depth profile of sample No.69

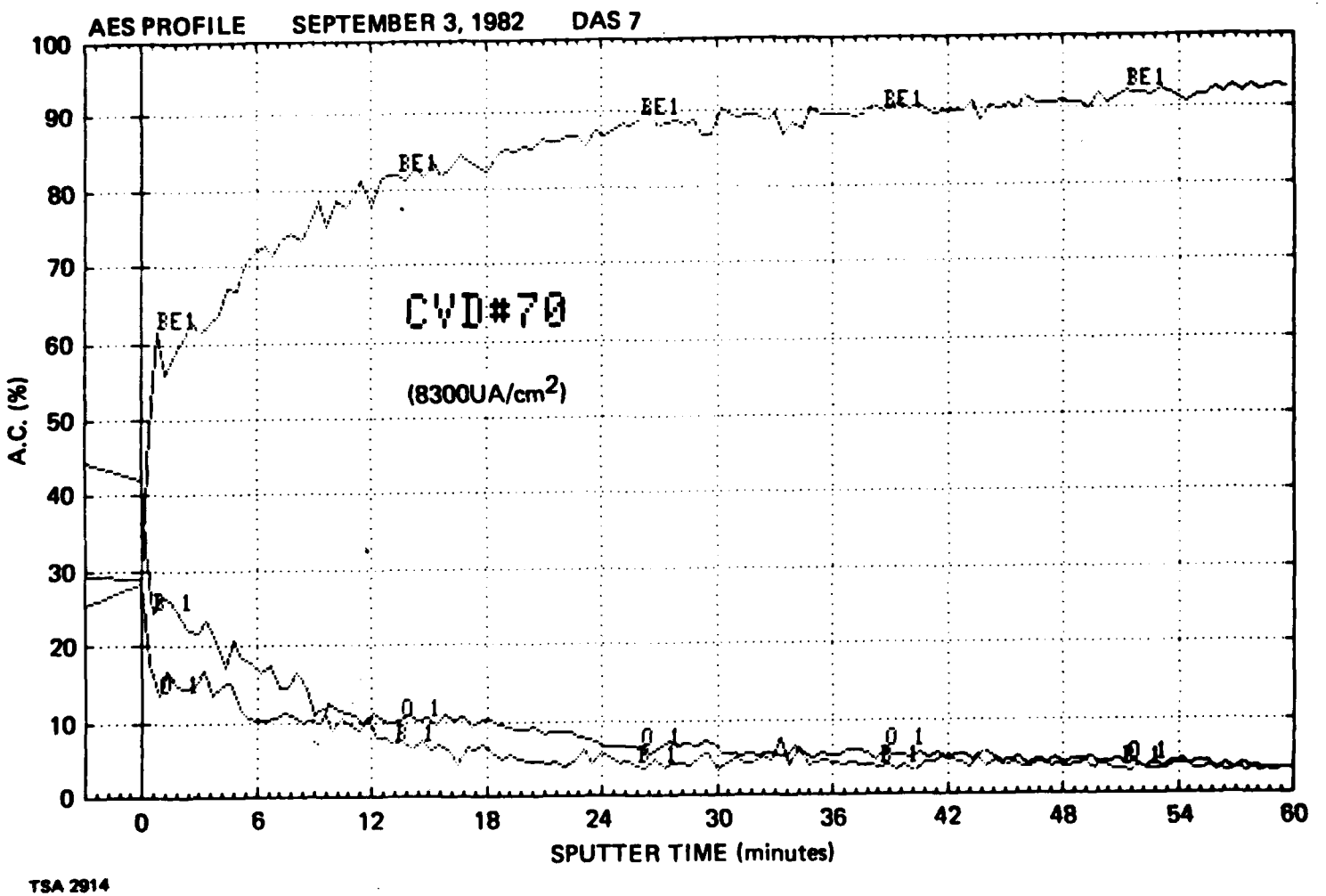

Figure 9. Auger depth profile of sample No. 70

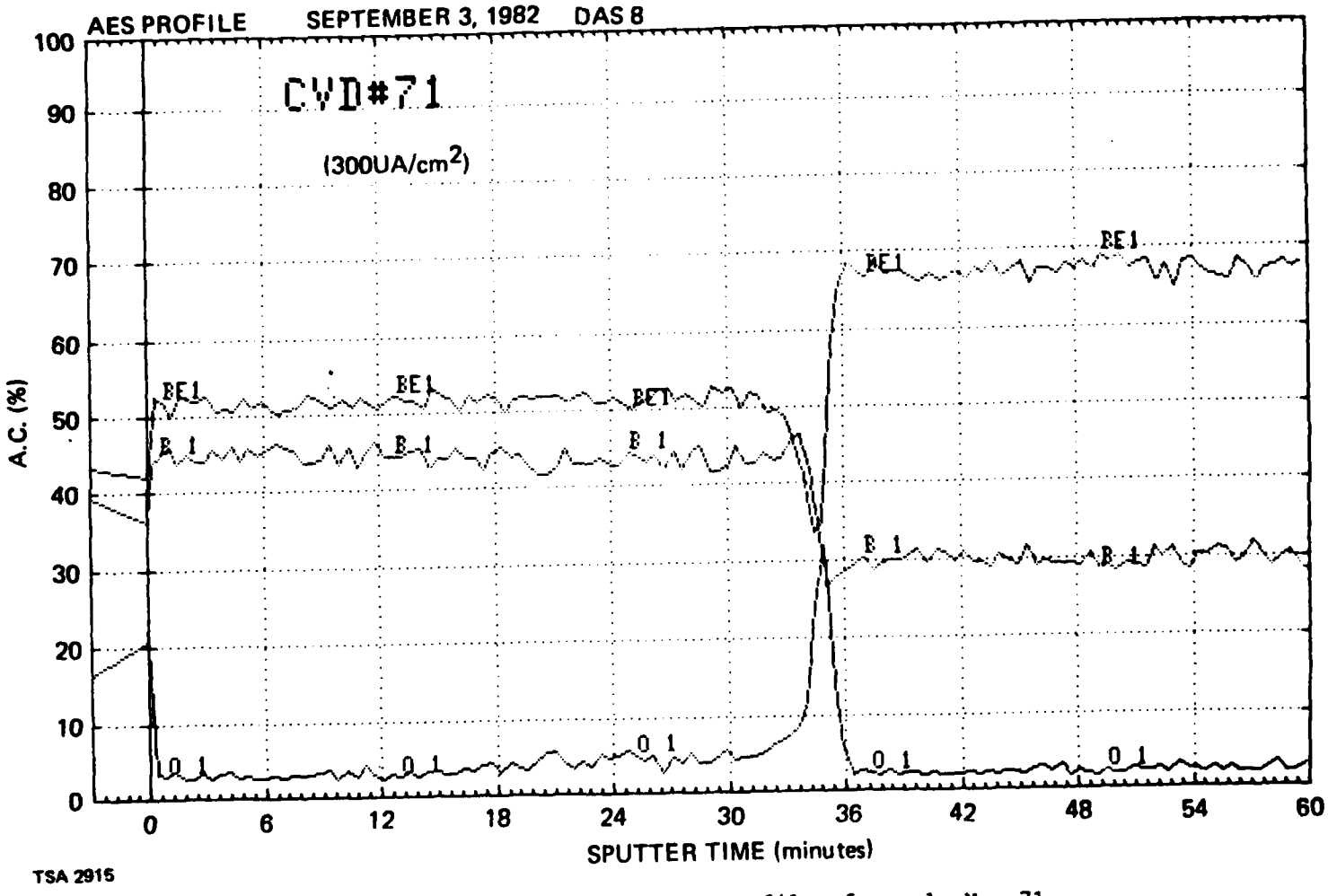

Figure 10. Auger depth profile of sample No. 71

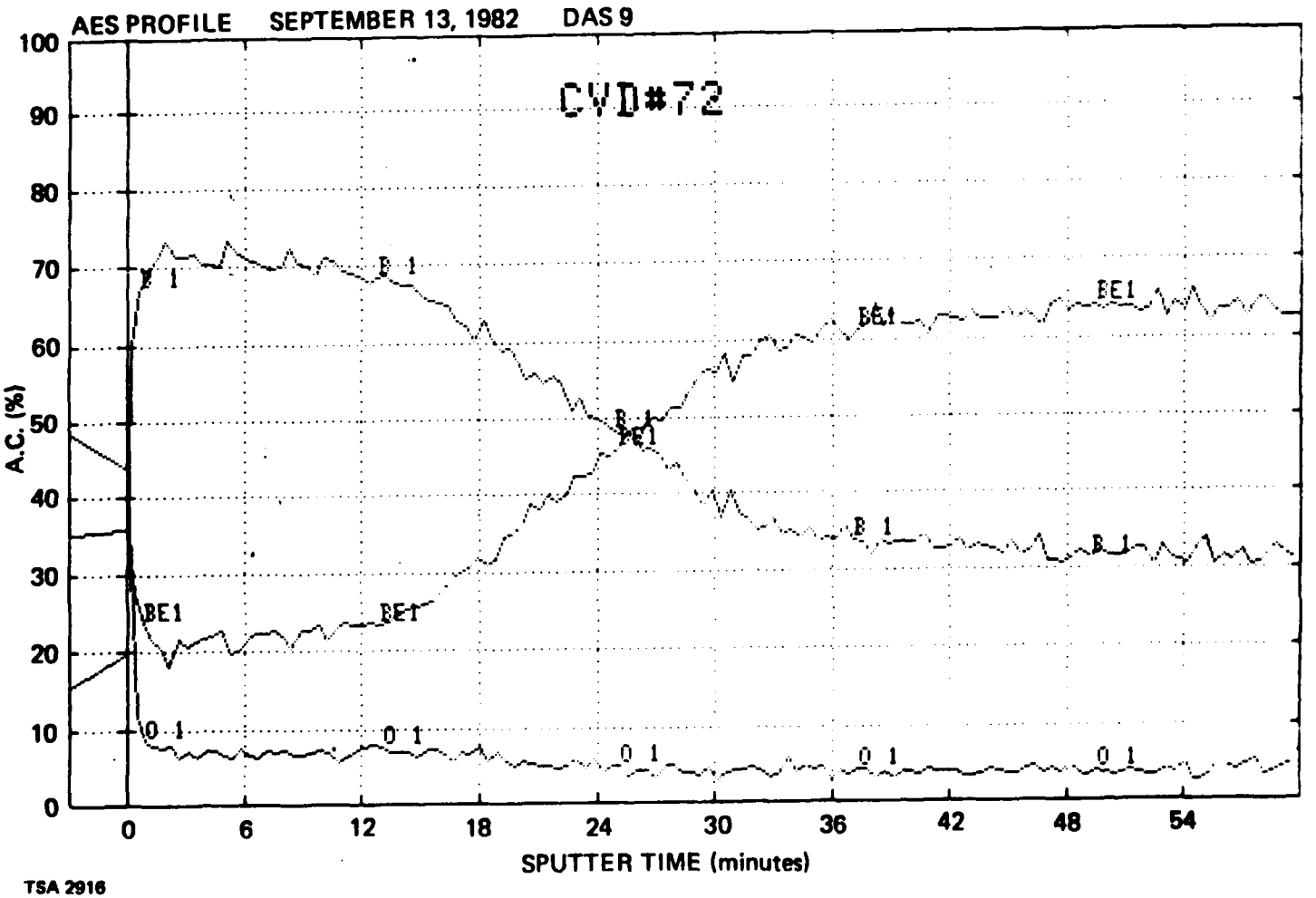

Figure 11. Auger depth profile of sample No. 72

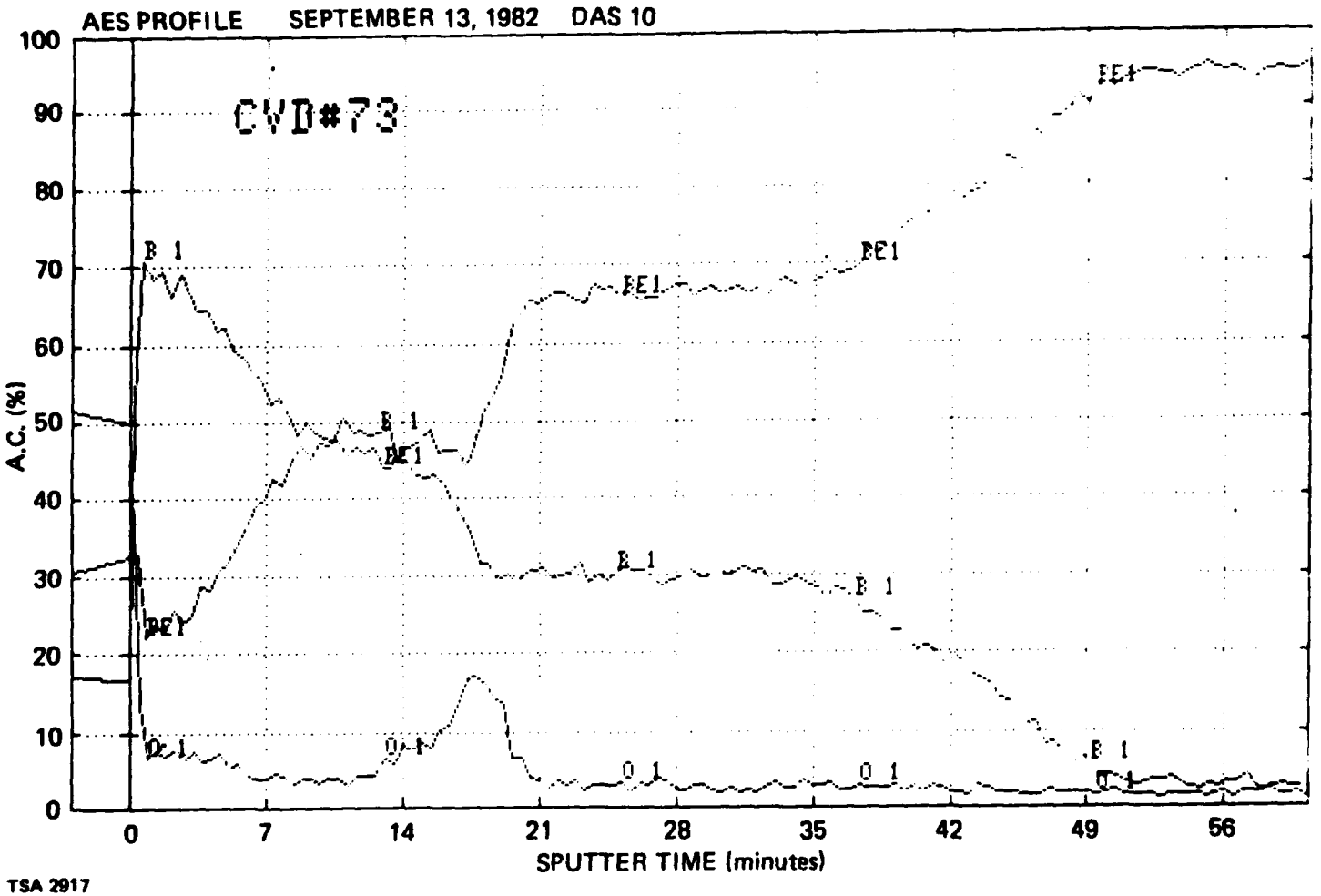

Figure 12. Auger depth profile of sample No. 73

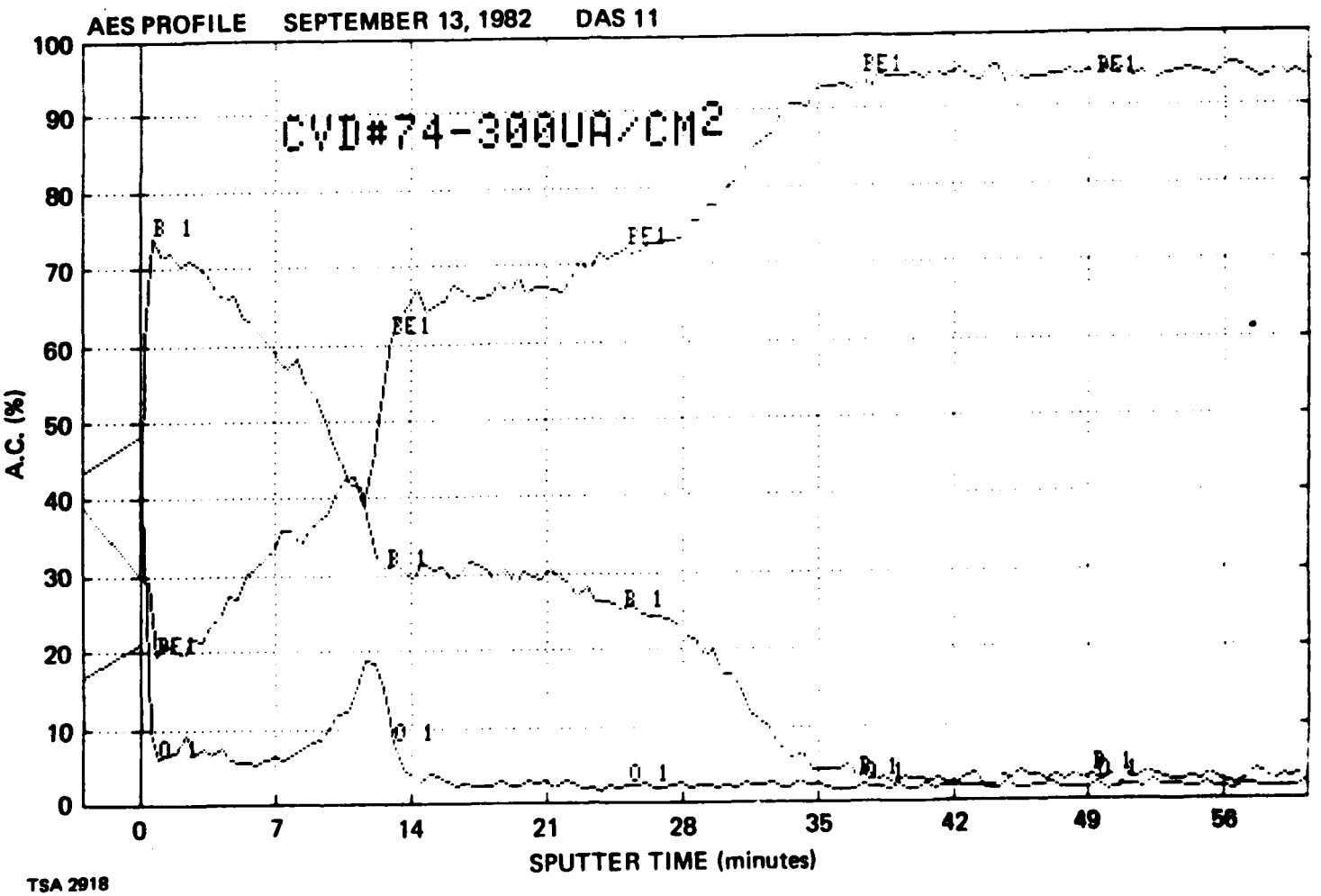

Figure 13. Auger depth profile of sample No. 74

Prior to Auger analysis, wear testing was performed on the samples. In order to provide a polished surface for the wear testing, approximately 2 μm of the film was removed by the polishing procedure. Therefore, the depth profile of each sample as presented in Figures 5 through 13 is incomplete. However, the chemical composition found at the beginning of the depth profile analysis is the chemistry of the surface on which the wear and friction tests were performed.

No attempts are being made to identify the phase compositions based on the chemical compositions for the time being. Some of the chemical compositions shown do not conform to the known intermediate phases. It is believed that these surfaces are composed of more than one phase. Microstructure analysis combined with the present Auger data will produce a better understanding, and should therefore be undertaken.

2.3.3 Fabrication of Gas Bearing Parts

For the initial trial, a gyro gas bearing has been selected, which happens to be a spool-type configuration. The complete bearing consists of a rotor, a shaft, and two thrust plates attached to the ends of the shaft. The two flat ends of the cylindrical rotor provide the mating surfaces for the thrust plates. For our first hardware experiment we have produced the CVD-coated beryllium thrust plates following the procedure similar to that of our sample number 69. The reason for selecting this particular film was that it showed good wear characteristics, fairly low friction coefficient, and a composition at the surface approximating a composition of BeB_2, which has the highest hardness values of all the compositions in the Be-B system. The CVD-coated thrust plates are now being prepared for assembling to form a complete bearing structure.

2.3.4 Personnel Safety Evaluation

Because of the high toxicity of diborane, a careful examination of the surrounding area, near the CVD apparatus, and the entire procedure including sample insertion and sample removal, etc., was made in collaboration with the Industrial Hygiene Department of the

Massachusetts Institute of Technology using the most up-to-date detection technique. The present apparatus and procedures therefore being used were found to be completely safe.

2.3.5 Further Studies

The results obtained thus far show the need for further studies in the following areas.

(1) Larger gas flow rates can be used at higher temperatures. Therefore, some further similar studies could be carried on at temperatures of 825° and 900°C for the CVD.

(2) Microstructure studies should be carried out in conjunction with Auger Electron Spectroscopy to obtain a clear understanding of the compositions and structures.

(3) The present CVD samples gave excellent results on both wear and friction against diamond pins, but rather disappointing results when used against a sapphire pin. This raises the question of compatibility of mating surfaces in a gas bearing. For the boron CVDed beryllium, several choices of mating surfaces are available, such as boron CVDed beryllium, beryllium-ceramic composite, ion implanted beryllium, pyroceram, and alumina. It will be very important to carry out such compatibility studies by wear testing using various pin and disc combinations.

SECTION 3

ION IMPLANTATION

3.1 Introduction

Ion implanted beryllium surfaces are being investigated as a means of producing hard, wear-resisting surfaces that have potential for gas bearing use. Case hardening or surface alloying of materials by this process is an emerging technology that has borrowed heavily from semiconductor electronic device fabrication, where the process is fully mature. While the basic concepts are similar, in practice the metallurgical modification of material requires much greater doses than are required to alter the electronic characteristics of a semiconductor. That difference and others makes this an exploratory effort, not only in the evaluation of results but also in the development of processing and testing procedures. The effort has so far concentrated on the implantation of beryllium using boron ions and a significant measure of success has been achieved with this binary alloy system.

3.2 Process Description

The ion implantation process differs from those based on diffusion by employing kinetic, rather than thermal, energy to introduce and emplace the foreign species which is intended to modify the host material. A high kinetic energy is given to the species to be implanted, such as boron, by first ionizing the boron and then accelerating the ions through an electrical potential difference. They are then directed as a beam or current of ions onto a substrate material, such as beryllium, whose surface their high kinetic energy allows them to penetrate. The quantity or dose of boron delivered is determined by the magnitude of the current and the length of time it is applied. The range of penetration of the ions depends on the accelerating potential. Consequently, for ion implantation processing, the concentration of boron in the surface of the beryllium is not limited by its solubility, and the penetration of boron into the

beryllium is not restricted either by the diffusivity of the boron or by the presence of a native oxide film on the beryllium. A principal feature of ion implantation is therefore the unique degree of control which it affords in generating alloyed surface layers.

3.3 Previous Work

Experiments performed on beryllium samples implanted with boron concentrations in the range of 10 to 40 atom percent at the Naval Research Laboratory (NRL) in a low current machine (so that the processing time requirement was inordinately long) showed that significant boron concentrations could be attained in the beryllium surfaces. Studies indicated that erosion due to sputtering was negligible and therefore did not set any serious limits on the concentrations which might be reached. These studies also demonstrated that increases in hardness values occurred with implantation. These values increased further when the samples were subjected to post-implant heat treatments.

Subsequent work on a second group of specimens, which were each of a size large enough to permit friction and wear testing after implantation, was performed in a new implanter with a higher current capability. These were implanted to levels of 60 and 40 atom percent boron in beryllium and again showed hardness increases. However, inconsistencies and a lack of reproducibility showed the need for better sample thermal control during implantation and examination of more than a single sample of a given type.

Much of the earlier friction and wear testing in this part of the program was done in a pin-on-disc format with pins made from 52-100 steel. The tests were performed on freshly cleaned surfaces without lubricants or coolants, as a means of ensuring well-defined and reproducible conditions. Perhaps because of the absence of any lubricating film, in many instances the steel pin material "crayoned" itself onto the disc surfaces resulting eventually in steel rubbing on steel. This occurrence, plus the desire to generate data with more direct engineering value, led to the recommendation that further wear and friction evaluation be performed with an aluminum oxide (sapphire)-tipped pin.

Microstructure evaluations of the implanted layers were attempted using reflection electron diffraction (RED) when it was realized that use of the transmission electron microscopy (TEM) and diffraction technique posed logistical problems. The results obtained by RED were termed inconclusive in that no clear diffraction pattern was obtained from the surface.

Subsequent RED examinations of as-polished, unimplanted beryllium also showed the absence of a diffraction pattern; however, the existence of a well-defined beryllium pattern was clearly observed when the unimplanted beryllium sample was stress relieved for one hour at about 790°C. This clearly suggested that the observed amorphous nature of the surface in the implanted specimens might well be the result of the sample preparation procedure that was adopted prior to implantation of the specimens and may or may not be related to the implantation of the boron species.

A variety of additional implants was performed. Included among these were flat, graded, and single-dose composition profiles. Analyses performed using Rutherford Back Scattering (RBS) and Auger Electron Spectroscopy (AES) showed that the desired profiles were obtained. (A reasonably good correlation was noted for the RBS and AES data.) Wear testing was performed on these many samples. A flex-pivot wear tester capable of both pin-on-disc and disc-on-disc testing was developed for this purpose. Experiments showed that for an identical peak surface concentration a flat boron profile was substantially superior in terms of resisting wear, compared to a graded boron distribution. This indicated that the wear mechanism was strongly influenced by what existed in the subsurface regions of the material in addition to the conditions in the immediate region of contact. Differences were observed in the friction traces of the implanted specimens compared to beryllium. A most notable feature was the existence of three distinct regions in the implanted materials, and these were attributed to effects resulting from gradual wearing off of the implanted layer.

3.4 Present Work

3.4.1 Sample Preparation

Additional implantations were performed on polished beryllium surfaces obtained on discs produced using the machining, stress-relieving, and lapping procedures discussed earlier.[9] Peak surface boron concentrations of 10, 20, and 30 atom percent were attempted for the several samples with a graded composition profile tailored into the subsurface regions. It was decided to explore these low-boron-containing compositions [lower than the 40 atom percent that is known to provide satisfactory results from earlier experimentation[10]] for purposes of minimizing the use of implanter time, thereby making the effort substantially more cost-effective. The graded compositions were also obtained for this same purpose.

Table 3 contains a list of the several samples that were implanted and the implantation parameters of significance. (These implantations are typically performed by exposing the beryllium sample to boron ion beams at successively lower energies.) The energy of the incident boron ions determines the depth of penetration of the ions into the beryllium surface (the higher the energy, the greater the depth) and the boron ion fluence (which is related to the current density at the substrate) determines the atomic concentration at a given depth. The energies used for this work were 25, 43, 67, 100, 140, and 192 keV and the fluences used for the 10 atom percent peak boron concentration sample corresponded to 7.1, 8.6, 8.8, 8.025, 6.25, and 3.775×10^{16} B/cm^2. The fluences used for the 20 and 30 atom percent samples, respectively, were two and three times the values of the 10 atom percent sample fluences. All of the implantation parameters were based on theoretically calculated values and the samples were subsequently analyzed for actual concentration levels and depth composition profiles using techniques such as RBS and AES.

Table 3. Parameters used for implantation of beryllium discs.

Specimen No.	Peak Nominal Concentration (atom percent)	Type of Implantation	Heat Sinking At Substrate	No. of Doses	Energy Range (keV)
7	10	graded	good	6	25-192
13	10	graded	good	6	25-192
14	20	graded	good	6	25-192
17	20	graded	good	6	25-192
12	30	graded	good	6	25-192

3.4.2 Chemical Composition and Profile Determination

Earlier results had demonstrated the AES technique to be quite capable of providing an adequate measurement of the boron depth profile in the sample.[8] This was established by comparing the AES-obtained results with data obtained using the RBS technique. It was determined, however, that the absolute measurement of the atomic concentration was more reliable using RBS than with information derived with the AES plots recorded on a chart paper. The instrumentation has since been upgraded on the AES machine and composition profiles were obtained during this reporting period using the software package supplied by the vendor. The data presented with respect to the AES work done on this new set of samples, therefore, includes information on the atomic concentration of the several elemental species.

3.4.2.1 Auger Electron Spectroscopy (AES)

Auger evaluation of the implanted materials was performed using a Physical Electronics machine. The machine was operated at 5 kV and the spot size of the incident electron beam was slightly less than 1 μm. Depth profiles were obtained by sputtering the sample with argon ions

and simultaneously examining the chemical composition of the material that was exposed to the incident beam at the various depths. The data were obtained in a form such that the atomic concentration of the several species of interest was plotted on the vertical (y) axis and the time of sputtering on the horizontal (x) axis. Since the rate of sputtering of the implanted layer was not known, it was not possible to directly convert the time of sputtering to the depth attained inside the sample by simple conversion of the data.

To more accurately determine the concentration profile, an alternate method can be followed.[8] This consists of measuring the depth of the groove (that was formed by sputtering of the sample surface) with a Sloan Dektak surface profilometer and assuming that the rate of sputtering is a constant throughout the sputtering period. A given fraction of the groove depth is then, therefore, equivalent to the same fraction of the sputtering time.

3.4.2.2 Results

Typical plots, obtained for peak-to-peak signal strength as a function of sputtering time (which is related to depth into the sample as discussed previously) are shown in Figure 14 for the 10 and 30 atom percent boron samples (numbers 13 and 12, respectively). The corresponding plots relating to atomic concentration versus sputtering time that were derived from the peak-to-peak values using the computer software are shown for these samples in Figure 15. It is clear that a close correlation exists between the data presented in either manner as would be expected.

The plots in Figures 14 and 15 show that whereas a composition gradient was obtained as intended in both of these samples, the peak boron concentrations at the surface were substantially larger than was expected on the basis of theoretically calculated values. These observations were similar to what was reported earlier,[8] where for an intended peak boron concentration of 40 atom percent, the actual value was close to 55 boron atom percent. The plots relating to sample 13

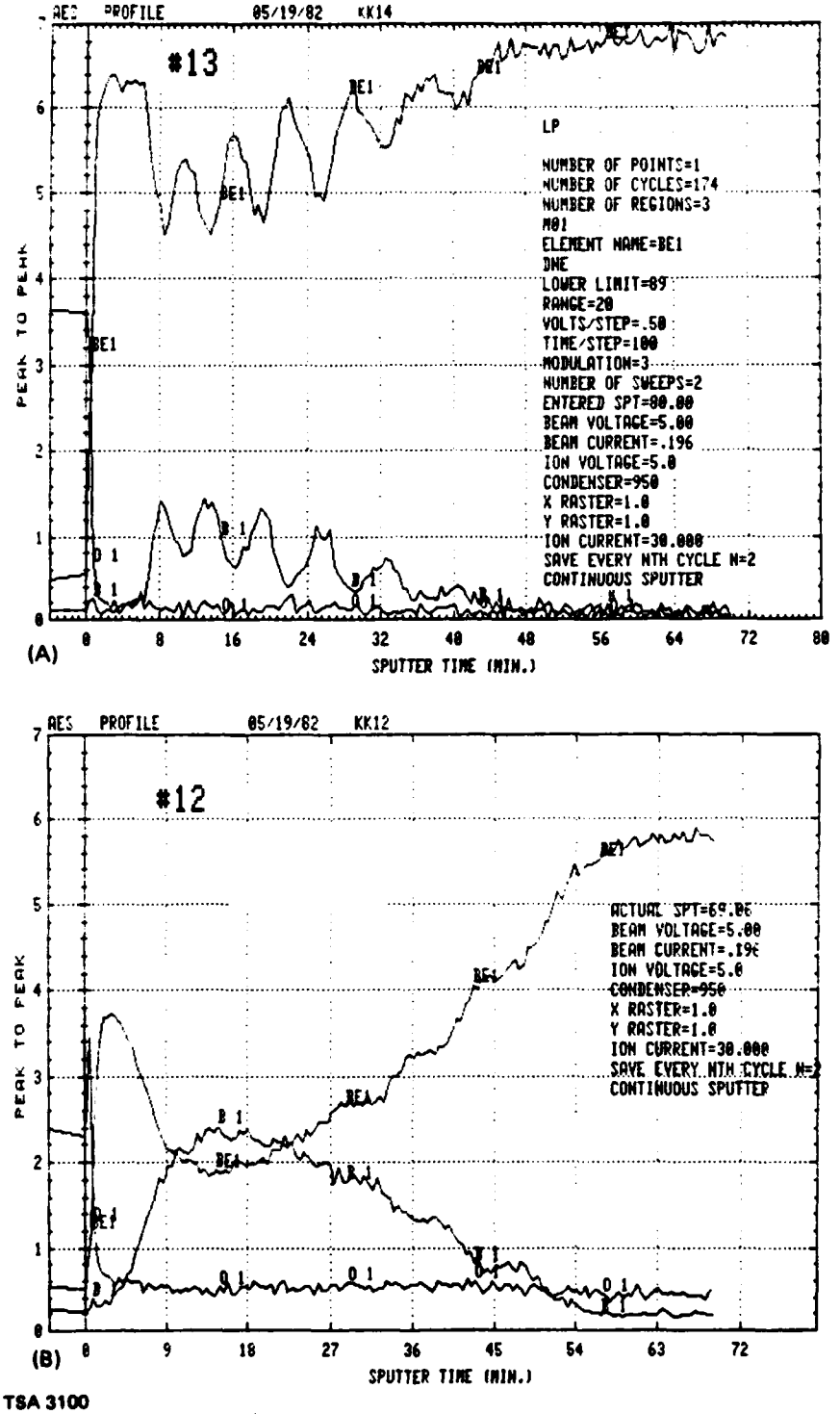

Figure 14. Plots of peak to peak signal strength versus sputter time for (A) Sample No. 13, and (B) Sample No. 12.

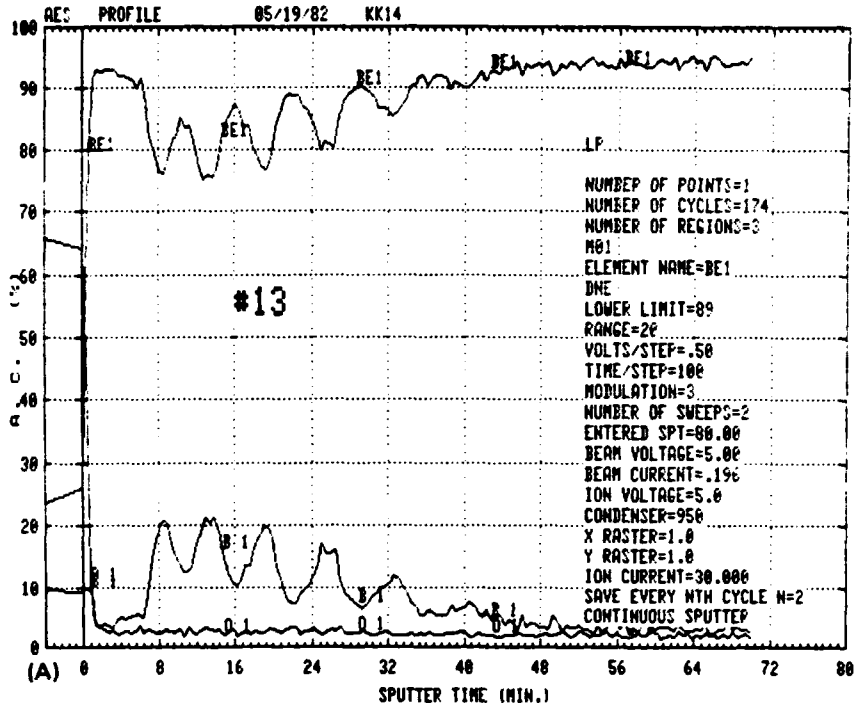

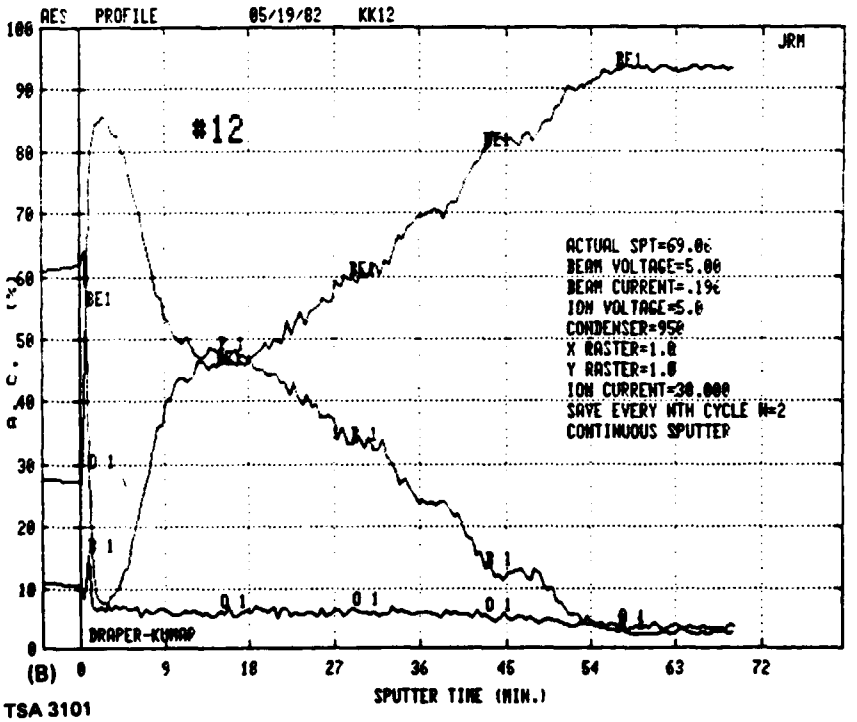

Figure 15. Plots of atomic concentration versus sputter time for (A) Sample No. 13, and (B) Sample No. 12.

were also composed of a nonuniformly decreasing boron concentration with increasing penetration depth. The composition profile was composed of what appeared as an overlapping set of gaussian-type curves, which are believed to be the result of the six different boron fluences that the sample was subjected to during its implantation with incident ion energies in the 25 to 192 keV range. When sample 7 was examined with AES to see if a similar situation existed, such was not determined to be the case. Two concentration depth profiles obtained on this sample are shown in Figure 16. The differences in the boron profile obtained at two different locations in the sample indicated that possible slight variations exist across the sample surface. The composition profile of this sample, however, was substantially more smooth than what was observed for sample 13, which had been processed under nominally identical conditions as sample 7.

An additional interesting observation was the lowered peak concentration value indicated for sample 7 compared to sample 13. This would seem to indicate that for a given fluence level, either the energy distribution of the boron ions incident on the sample surface was broader for sample 7, or the broadened overlapping peak observed for number 7 resulted from thermally activated phenomena such as a slight rise in temperature (over that encountered in sample 13) during the implantation process. This in turn would mean that better cooling was provided to the substrate of sample 13 while the implantations were performed.

3.4.3 Friction and Wear Testing

All of the testing was performed with the CSDL-designed flex pivot wear-tester that was described in detail in Reference 8. This apparatus was designed for maximum adaptability and is capable of performing both pin-on-disc and disc-on-disc type of wear tests. Loading can be varied from a few grams to 10 kilograms by means of either dead weights or a pneumatic loading device. A signal generator coupled to an elastic flex-pivot provides a continuous torque signal from which the value of the friction coefficient can be calculated. Test speed can be varied from 100 to 1200 r/min. This test equipment is installed in a beryllium hood to permit tests on beryllium.

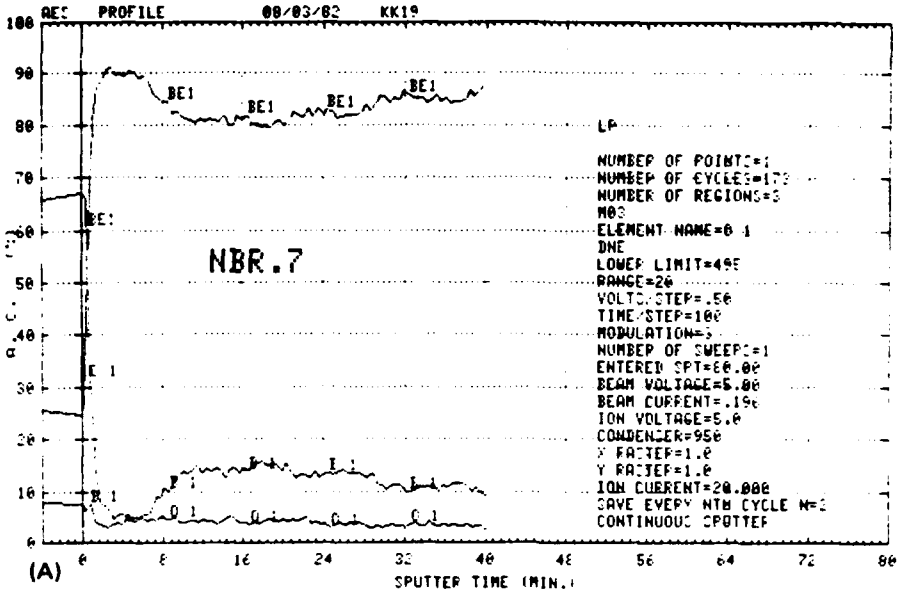

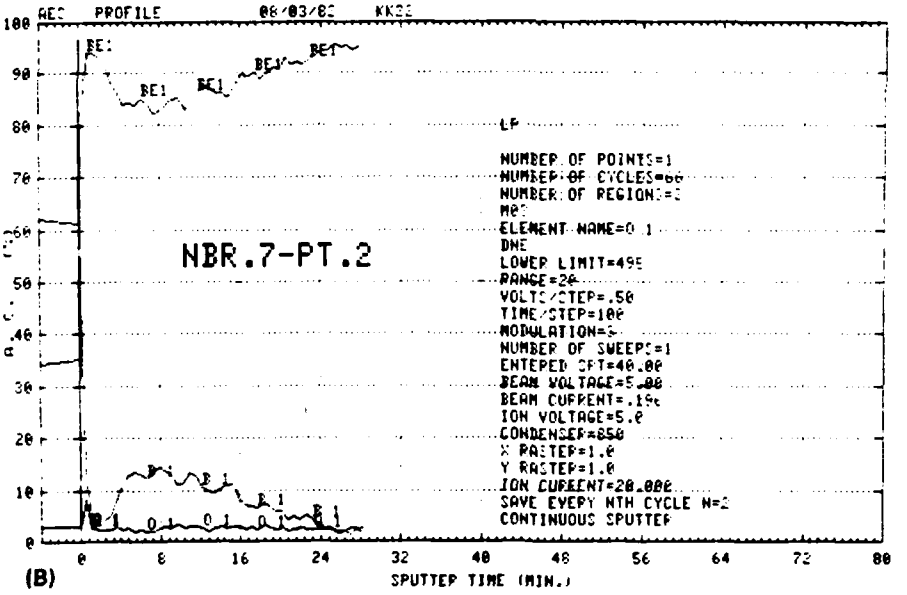

TSA 3102

Figure 16. Atomic concentration profiles for sample No.7.

Experiments performed earlier, using this wear-testing apparatus, on unimplanted beryllium and beryllium implanted with flat and graded profile boron concentrations (with peak concentrations of 40 atom percent boron) had shown a remarkable improvement in wear resistance from the implantation process. These studies had also shown interesting features associated with the friction traces that were obtained on the implanted surfaces. Traces obtained at low loads showed little variation of the friction coefficient with time. These traces were somewhat similar to those obtained on polished unimplanted beryllium except that the traces on the latter indicated a substantially larger stick slip behavior and the friction coefficient value was much larger for the unimplanted sample. The friction traces obtained at the higher loads on these samples, however, showed a marked deviation from the flat-type (constant value) trace observed for beryllium and for the implanted specimens measured at the low loads. In these cases, three (almost distinct) regions were indicated on the friction trace. These were interpreted as corresponding to a region A with low/no wear (friction coefficient constant), a region B with rapidly increasing wear as indicated by the accompanying increase in the friction coefficient, and a steady-state wear region where the friction coefficient value increases quite gradually. Both regions A and B were found to shrink with increases in applied loads. Because of the nature of the traces obtained during these evaluations, it was considered important to calculate and record the measured value of the friction coefficient at different points in time during a 10-minute run.

Wear-test experiments (using a 1/8-inch-diameter sapphire ball as a pin) have also been performed on beryllium samples implanted with graded boron concentrations having the intended peak boron composition values of 10, 20, and 30 atom percent boron. It was hoped that in conjunction with the results obtained earlier on the 40 atom percent samples, a peak boron concentration dependence of the friction and wear behavior might become evident through such an evaluation.

The data obtained on these several samples are shown in Tables 4 through 6. As discussed earlier, the data were once again tabulated for different times to compare the time-dependent rise in the value of the friction coefficient for these samples. For purposes of comparison, the friction coefficient data for the 40 atom percent boron flat and graded profile specimens are reproduced in this report and are shown in Tables 7 and 8. The data are somewhat ambiguous in that no clear dependence of friction data [which are also believed to be related to wear behavior by virtue of the interpretation of the friction traces discussed in the last report[8]] was observed for these several specimens. Per our earlier experience and in agreement with our interpretation of the measured friction data, the initial friction coefficient value as observed after 0.1 minutes of testing time, with an applied load of 20g, appeared similar for all of these samples. In fact, similar initial values were also observed for the flat profile 40 peak atom percent boron specimen discussed in last year's annual report and shown in Table 7. The friction data for the graded profile 40-VII sample in Table 8 was more erratic from run to run; however, an average value of the set of the four 20g-load runs on this sample is reasonably consistent with what was observed on all of the other samples for the 0.1-minute friction value.

Further examination of the data in Tables 4 through 8 shows that, in general, the performances of the 40 and 20 peak atom percent samples were superior to the 10 and 30 atom percent samples in that a slower rise in the average value of the 20g load runs was indicated for sample numbers 40-VII and 14 compared to samples 13 and 12. This is clearly observed by the data tabulated at different points in time which reflect the time-dependent changes observed in the friction traces. Therefore, no clear dependence of the friction (and thereby wear) behavior is observed on the peak concentration value of the graded profile boron implanted specimens. Among all of the specimens investigated it is clear that the 40 atom percent boron flat profile specimen behaves in a superior fashion.

TABLE 4: Friction coefficient data on NRL sample 13 (10%B) calculated at different times

RUN No.	LOAD (g)	TIME (MINUTES) 0.1	1	3	5	10
1	20	0.15	0.22	0.31	0.37	0.46
2	20	0.15	0.20	0.26	0.29	0.46
3	20	0.13	0.20	0.26	0.29	0.37
4	30	0.13	0.26	0.35	0.44	0.48
5	40	0.31	0.70	—	—	—
AVERAGE VALUES OF 20 g RUNS		0.14	0.21	0.28	0.32	0.43

4/82 CD27261 REV A 5/83

TSA 3109

TABLE 5: Friction coefficient data on NRL sample 14 (20%B) calculated at different times

RUN No.	LOAD (g)	TIME (MINUTES)				
		0.1	1	3	5	10
1	20	0.15	0.20	0.24	0.31	0.35
2	20	0.15	0.20	0.24	0.26	0.31
3	30	0.13	0.20	0.24	0.29	0.42
4	40	0.18	0.26	0.33	0.37	0.51
AVERAGE VALUES OF 20 g RUNS		0.15	0.20	0.24	0.29	0.33

4/83 4/82 CD27259 REV A 5/83

TSA 3110

TABLE 6: Friction coefficient data on NRL sample 12 (30%B) calculated at different times

RUN No.	LOAD (g)	TIME (MINUTES)				
		0.1	1	3	5	10
1	20	0.15	0.29	0.40	0.40	0.44
2	20	0.13	0.26	0.40	0.42	0.44
3	20	0.13	0.22	0.40	0.46	0.62
4	30	0.15	0.37	0.77	0.86	—
AVERAGE VALUES OF 20 g RUNS		0.14	0.26	0.40	0.43	0.50

4/82 CD27260 REV A 5/83

TSA 3111

TABLE 7: Friction coefficient data on NRL 40-IV; calculated at different times

RUN No.	LOAD (g)	TIME (MINUTES) 0.1	1	3	5	10
1	20	.13	.13	.15	.22	-
2	20	.11	.11	.13	.20	-
2	20	.20	.20	.26	.35	-
4	20	.15	.15	.22	.35	-
5	20	.13	.11	.15	.22	-
6	20	.18	.18	.20	.31	-
7	45	.13	.20	.33	-	-
8	45	.18	.22	.48	.66	.90
AVERAGE VALUES OF 20 g RUNS		0.15	0.15	0.19	0.28	-

4/82 CD27085 REV A 5/83

TSA 3112

TABLE 8: Friction coefficient data on NRL 40-VII; calculated at different times

RUN No.	LOAD (g)	TIME (MINUTES 0.1	1	3	5	10
1	20	.07	.11	.11	.11	.20
2	20	.26	.31	.35	.46	.48
3	20	.22	.29	.29	.33	.37
4	20	.09	.13	.13	.18	.20
5	45	.24	-	.40	.55	-
6	45	.26	.31	.40	.55	-
AVERAGE VALUES OF 20 g RUNS		0.16	0.21	0.22	0.27	0.31

4/82 CD27090 REV A 5/83

TSA 3113

In addition to the interpretation of the wear behavior of the implanted surfaces from the friction traces that were obtained, our earlier work had also shown that optical microscopy was quite helpful in determining when severe wear occurs. The micrographs obtained from the wear tracks of the 10, 20, and 30 atom percent boron samples from the several runs performed at different applied loads are shown in Figures 17 through 19. By comparing the resistance of the implanted surface to severe wear as indicated by the broad wear tracks obtained, for instance, in the 10 and 30 atom percent samples at a 30g load to the much less severe wear marks observed for loads up to 40g in the 20 atom percent sample, it is clear that the 20 atom percent sample shows substantially greater wear resistance than do the other two samples. The results inferred from an examination of these micrographs are clearly in agreement with what was concluded from the friction data.

It is widely believed that the hardness of the surface is an indication of its wear resistance; therefore, the higher the hardness, the greater is its wear resistance. Microhardness measurements were made on several of the samples that we have discussed and the Knoop indentation values of microhardness, expressed in kg/mm^2, are shown in Table 9. It is difficult to measure the hardness of such thin surface films accurately, both at high applied indentation load (because the substrate contribution is excessive) and at very low load (where the surface contribution dominates but questions arise with respect to "the actual" as compared to "the intended" load). We have, therefore, devised a procedure whereby microhardness measurements are made in a range of applied loads and the variation of microhardness as a function of applied load gives a more reliable assessment of the hardness of the surface.[11] Conventional thinking with regards to the relationship of surface hardness to its wear behavior notwithstanding, the data in Table 9 show that the wear behavior of these samples cannot be explained on the basis of the microhardness data obtained in this effort.

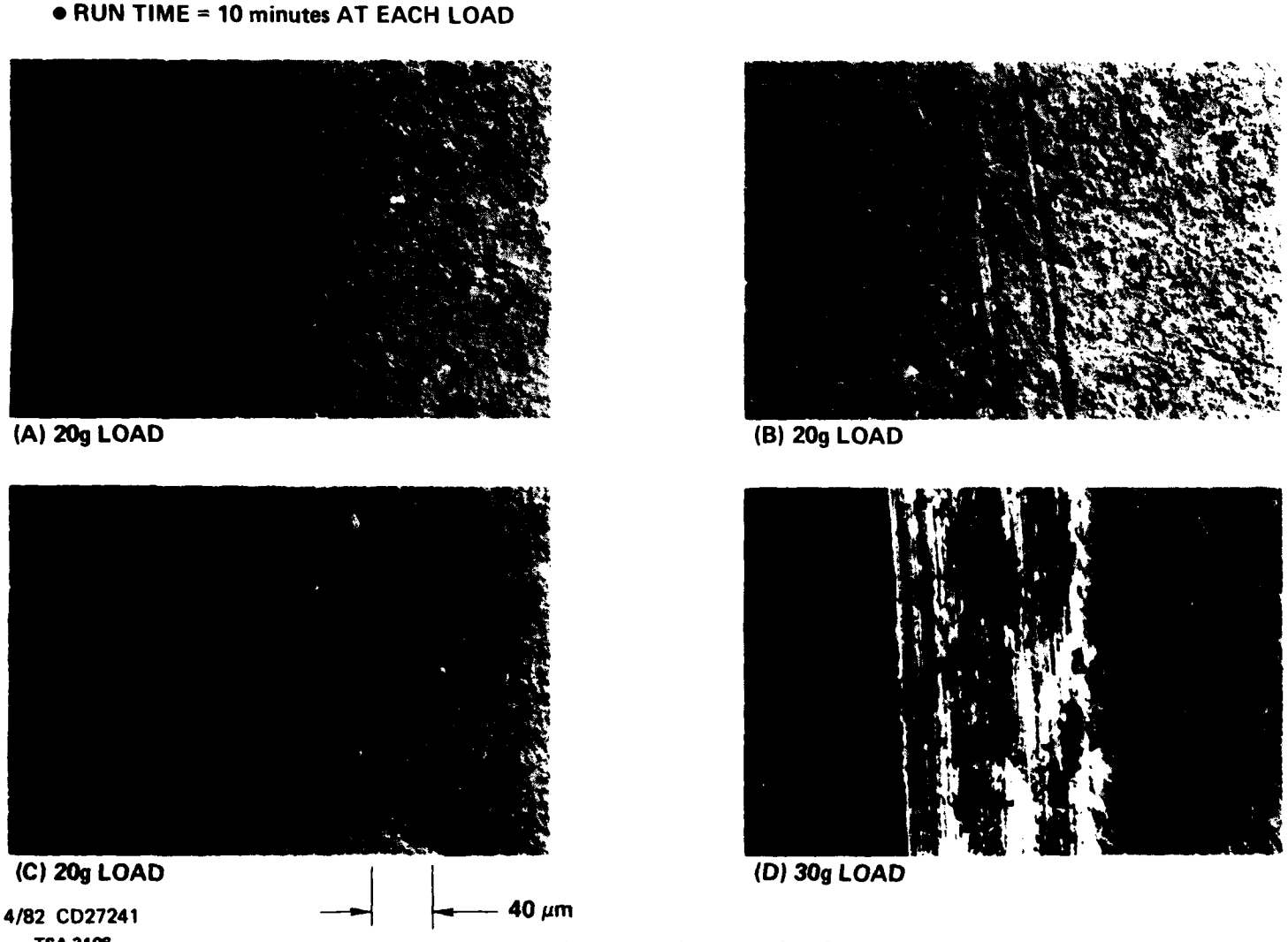

Figure 17. Sample 13 (10% B) micrographs from wear tests. Wear tracks made at different loads.

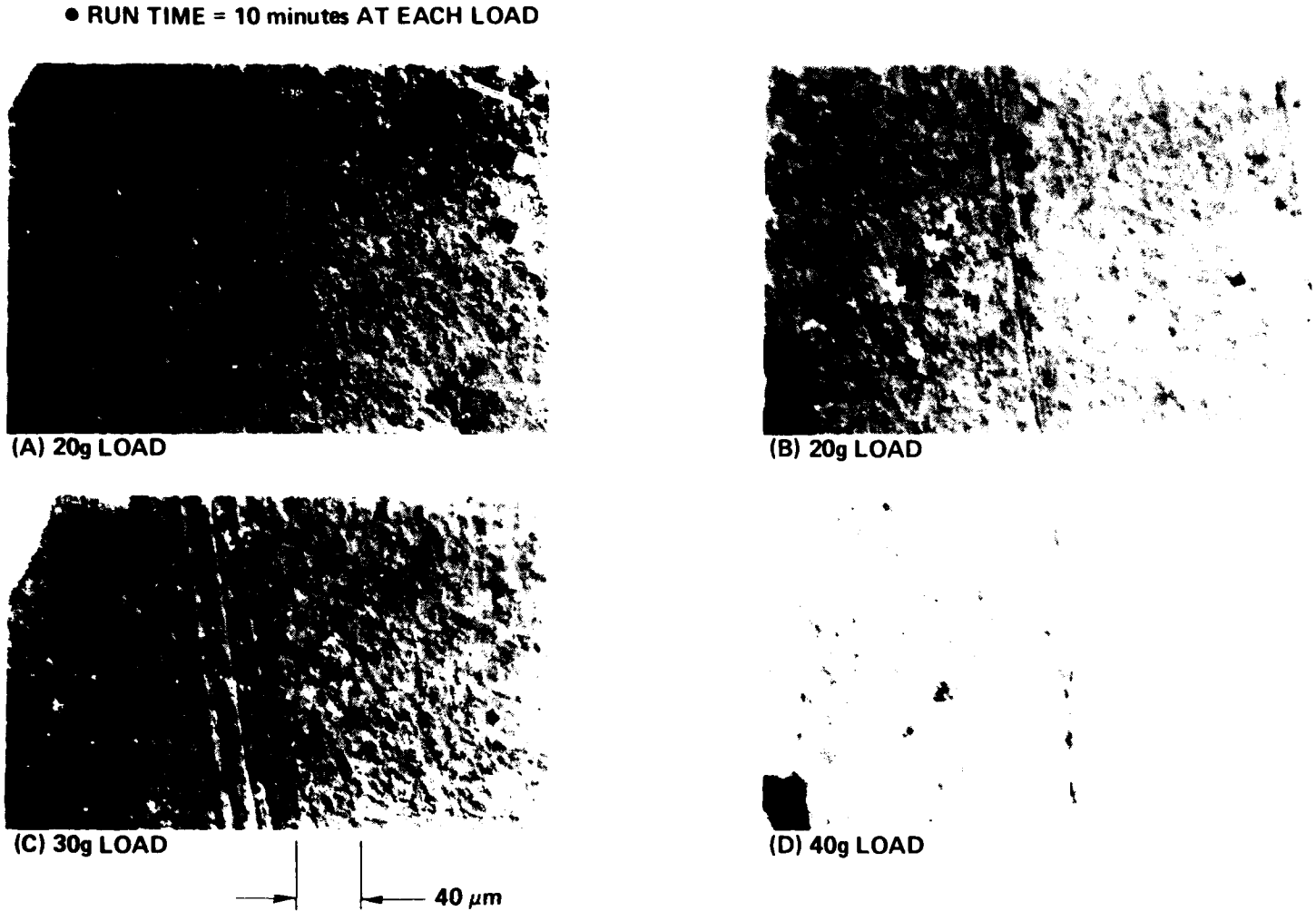

Figure 18. Sample 14 (20% B) micrographs from wear tests. Wear tracks made at different loads.

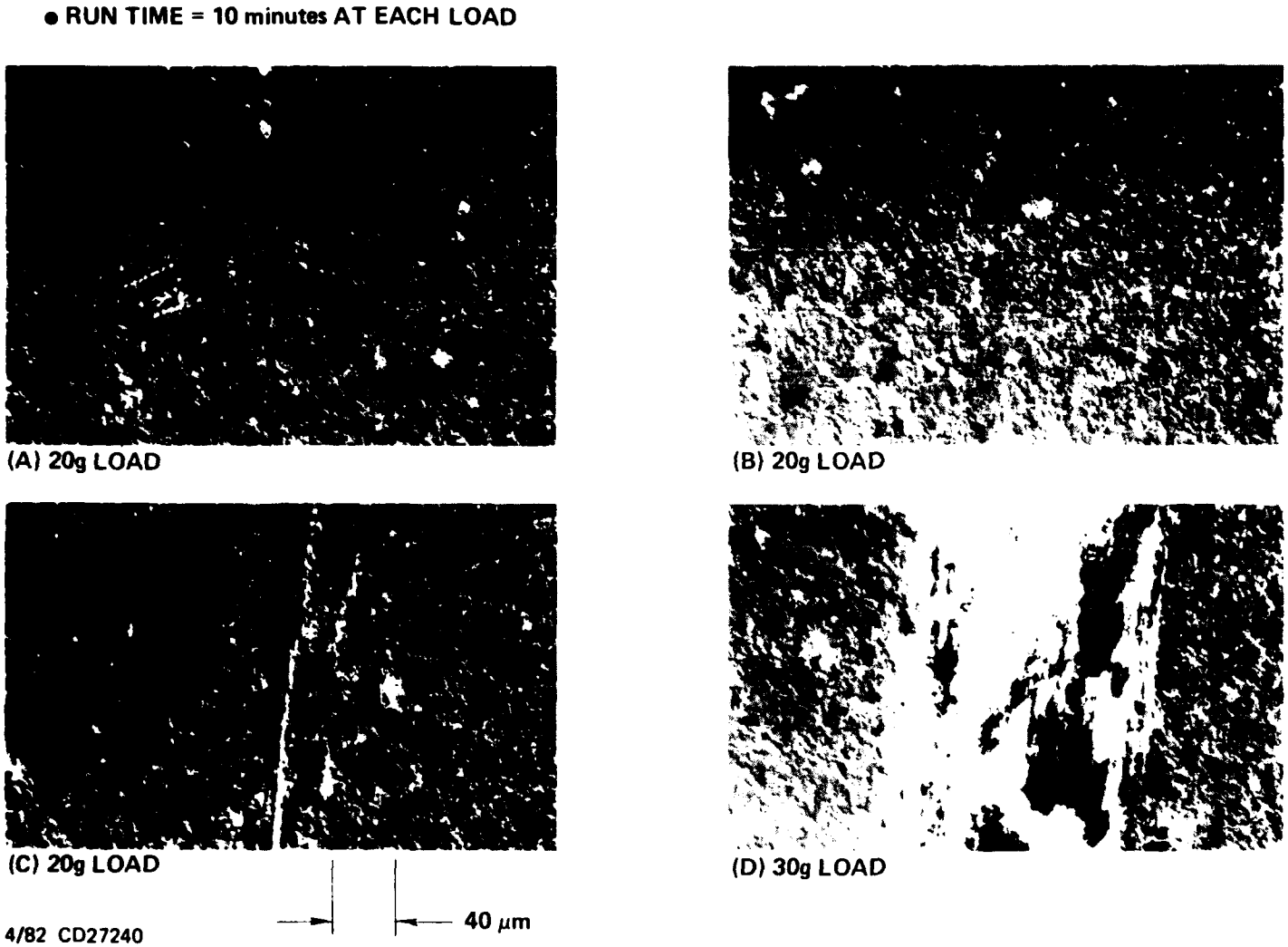

Figure 19. Sample 12 (30% B) micrographs from wear tests. Wear tracks made at different loads.

Table 9. Microhardness readings average khn (Kg/mm^2) on several NRL implanted samples

APPLIED LOAD (g) \ SAMPLE	40-IV (UNIFORM)	40-VII (GRADED)	NUMBER 12 (30% B)	NUMBER 14 (20% B)	NUMBER 13 (10% B)
50	356	341			
25			390	381	372
10	542	762	686	643	703
5	1153	1211	1184	1017	1123
2	1965	2233	1622	1682	1736

4/82 CD27216 REV A 6/83

3.4.4 Hardware Fabrication and Evaluation

Because the wear test experiments performed to date have shown that the 40 atom percent, flat boron profile gives the best results, two beryllium discs, with grooves in place, were implanted with this concentration and profile to examine the industrial applicability of the implanted surfaces in actual gas bearing use. These two discs constitute the thrust plates of a conventional spool-type gas bearing. To minimize the number of variables, all of the other structural members, including the rotor and the journal were selected from existing hardware with only the boron-implanted thrust plates comprising the change. The bearing was assembled unlubricated, in contrast to the conventional bearing which has a lubricant applied to its rubbing surfaces prior to evaluation and performance, and tested as a gas bearing. The response of this modified gas bearing was very satisfactory during the initial evaluation with respect to start-up and touchdown characteristics. When the bearing was examined for life test performance in regard to repeated start-stop cycles, the bearing was observed to fail after a few cycles. When the bearing was disassembled for inspection, it was discovered that the failure was related to removal of a small chip of the anodized surface of the journal. The implanted thrust plates looked as good as new. A new set of parts was subsequently received and work was initiated for assembling the bearing in a like manner with the same thrust plates in the hope that a satisfactory test will result from this repeat effort.

3.4.5 Additional Related Investigations and Future Work

Electron microscopy data obtained at NRL provided conclusive evidence of second-phase formation in boron-implanted beryllium samples.[10] The diffraction results suggested that more than one beryllium boride phase was possibly present. Since the temperature during implantation was intentionally held at low values, the increased boron mobility, as indicated by the occurrence of precipitate formation, was in all likelihood the result of irradiation-enhanced diffusion. The presence of a multitude of phases might well have been the result of compositional variations in the implanted specimens.

Two beryllium discs that were mailed earlier to TRW, Inc. for thermal energy implant of boron were received for further evaluation. These discs are currently being examined for boron dose and profile using the RBS technique at NRL, after which they will be returned to CSDL for AES and friction and wear evaluation. Two additional beryllium discs are also awaiting implantation of carbon and nitrogen ions, respectively, along with boron, to generate boron carbide (B_4C) and boron nitride (BN) stoichiometries in the beryllium surface. It is possible that these surfaces might possess higher load bearing capability during the wear tests than what has so far been demonstrated for the boron-implanted surfaces. Additional work is also planned on samples with the binary Be-B compositions, primarily from the view of examining the effects of low temperature heat treatment on the tribological behavior of the implanted surfaces.

SECTION 4

COMPOSITE MATERIAL

4.1 Introduction

Beryllium-ceramic metal matrix composites fabricated by hot isostatic pressing of blended powders are being examined as an alternate approach to the fabrication of hard, wear-resisting surfaces for use in gas bearings. Beryllium has served as the metal matrix in these components because of its very desirable bulk properties. The physical properties of a composite made from this metal are, therefore, expected to be more compatible to the rest of the gyro structural members than those either of a solid ceramic or of a composite fabricated using other metal constituents as the host material. It is anticipated that the physical characteristics of these composites will be between those of ceramic and beryllium. The benefits in using this type of material lie in the recognition that the entire wear and friction process is confined to the ceramic particles standing out in relief at the surface of the composite.

4.2 Previous Work

4.2.1 Material Selection

The criteria that were used to select ceramic powders for fabricating these composites included the following:[12]

(1) Microhardness

(2) Chemical stability

(3) Thermal expansion compatibility

A ceramic with a high value of microhardness was desired principally because hard materials are known to be resistant to degradation from processes such as impact and erosion and also because these display relatively low values of the coefficient of friction.[13]

Chemical stability, as indicated by the values of the free energies of formation of the several compounds, is of concern during consolidation because even though it is important that the metal matrix wet the ceramic, one does not want the metal to chemically reduce the ceramic at the temperature used for densification.

Thermal expansion compatibility consideration involves selection of a ceramic with an expansion coefficient only slightly lower than that of the surrounding metal and this leads to a mild compressive state of stress around the particle. An expansion coefficient higher than the metal will cause the ceramic particles to pull away from the metal during cooling after hot consolidation whereas one considerably lower will result in a very high level of stress.

4.2.2 HIP Process Development

Beryllium-titanium diboride composite material fabricated during initial experiments at CSDL using the hot isostatic pressing technique demonstrated that the fabrication sequence in itself needed a certain amount of development effort.[14,15] Poor densification was obtained in a sample that was isostatically densified at 900°C and 15 klb/in^2 gas pressure for 2 hours. Large pockets containing loose TiB_2 powder (which was the chosen ceramic) were observed with the unaided eye.

This problem was substantially corrected by resorting to high-energy powder blending (in a ball mill), outgassing of the powders at 600°C prior to container encapsulation, and using a higher densification temperature of 950°C.

4.2.3 Composite Development

Based on the selection criteria outlined above, the ceramics Al_2O_3, TiC and TiB_2 were chosen for further examination. Beryllium powder designated as -325 mesh was blended with powders of these different ceramics using the high energy blending procedure discussed previously. The variations that were attempted pertained to type, percent volume, and particle size of the ceramic. The blended powders were cold and, subsequently, hot isostatically pressed at 975°C for 4 hours under an inert gas pressure of 15 klb/in^2.

Lapping studies performed on coarse TiB_2-containing composites showed that use of coarse (500-grit-size) particle Al_2O_3 as the polishing compound resulted in the ceramic particles standing out considerably in relief above the beryllium surface. Scanning Electron Microscopy (SEM) observations showed that the surface of the recessed beryllium after polishing with coarse particles was also quite rough. When this sample was subsequently polished with the finer Al_2O_3 pastes (the finest contained a 2- to 3- micron Al_2O_3 particle size), micromachining of the TiB_2 particles was observed. The recessed beryllium also had a smoother surface in these instances.

Observations related to effects of ceramic particle size indicated that the -325-mesh TiB_2 particle-containing composites were more desirable than were the 1- to 2-micron-containing composites. While the -325-mesh samples showed a reasonably uniform distribution of the particles throughout the beryllium matrix, the 1- to 2-micron TiB_2 particulate samples showed that the ceramic particles were mainly segregated at the grain boundaries of the beryllium. Micromachining effects on the ceramic particles were not observed in the 1- to 2-micron samples, possibly because of their very small particle size, and maybe even because of a lowered tendency of the particles to remain bonded to the matrix.

These studies concluded that of the different ceramics investigated, TiB_2 was the most promising and should be examined in greater detail. TiC containing composites were much too porous, an effect attributed to outgassing problems associated with the ceramic powders prior to encapsulation and high temperature HIP. The problems with Al_2O_3 on the other hand, were related to inadequate bonding of the particles to the surrounding beryllium matrix resulting in particle pull-out during polishing.

4.2.4 Composite Investigations

Reasonably extensive hand-held lapping procedures (primarily using diamond containing compounds and diamond impregnated commercially procured Abernathy laps) were investigated with the purpose of producing well-polished TiB_2 surfaces in relatively short time. It was noted that severe damage (which were observed as pits) resulted in the ceramic particles from contact with the diamond particles. When polishing using fine particle (0.05 μm) Al_2O_3 was attempted on these surfaces, gradual removal of damage was observed; however, this was obtained at the expense of producing a considerable amount of ceramic particle relief at the surface. This problem was substantially minimized when Syton (a commercially available ultrafine particle SiO_2 suspension) was used as the polishing medium.

Wear tests were performed on the as polished surfaces. A disc-on-disc format for wear testing was examined and quickly discarded when extensive cocking problems were encountered. Pin-on-disc experiments were subsequently attempted using both TiB_2-composite and sapphire pins with different radii of curvature. Problems were encountered with the composite pin because it was flat. A curvature was subsequently placed on the edge of the composite pin. Wear tests with the sapphire pins always resulted in crayoning of the sapphire on the composite surface giving rise to a build-up of material as indicated by a surface profilometer.

Experiments were also initiated towards the fabrication of composites with different particle sizes of the ceramic and towards how the production of composite parts in near-net shape and size. Efforts were made at examining the industrial application of the TiB_2-containing composites. Initial evaluations were very encouraging and these results served as a basis for a substantially more expanded wheel build and evaluation effort at a vendor's facility under a separately funded government program.

4.3 Present Work

In the last annual report,[8] work was reported to have been initiated on the fabrication of TiB_2-based composites containing different sizes of the ceramic particles. Size classifications were performed using an Alpine American Corporation 100 MZR unit and size ranges corresponding to -10, -20 +10, -30 +20, and +30 μm were obtained. (A minus sign indicates particles less than the size in μm and a plus sign indicates particles greater than the stated size. For example, a -20 +10 μm size fraction implies that the particles are greater than 10 μm, but smaller than 20 μm).

The different ranges of classified powders were subsequently blended with -325-mesh beryllium powder (using techniques that were developed earlier) to give identical compositions of 45 volume percent ceramic. The blended powders were cold isostatically pressed in rubber boots, then encased in low carbon steel cans, and HIPed at 1000°C and 30 klb/in.^{2} argon gas pressure. Similarly sized beryllium powder could not be obtained commercially, mainly because it is difficult to handle beryllium owing to its toxicity in fine particle form. Also, because the different beryllium size ranges were expected to contain different levels of beryllium oxide, which would represent an additional variable (aside from the different TiB_2 particle size range) in the overall experimentation, this option was not considered to be of paramount importance in the structural optimization of the composite.

4.3.1 Development of Microstructure

Lapping procedures, investigated and reported earlier, were further developed to produce nearly damage-free microstructures. The successful procedure consisted of the following lapping steps. (In each case the lapped specimen was cleaned ultrasonically in Freon. All of the lapping was performed inside a hood specifically dedicated to the polishing of beryllium surfaces).

(1) One-hour lapping with 45μm diamond paste followed by an additional one-half hour lapping with 15μm diamond paste.

(2) One-half hour exposure to a 600 mesh diamond-impregnated lap followed by thirty and ten minute lapping treatments using 3μm and 1μm diamond pastes respectively.

(3) Polishing of the preceding surfaces on a standard polytex rotating wheel using Syton suspension.

The surfaces obtained with these procedures were substantially superior to what were reported earlier. Photomicrographs obtained on the surfaces of the -10 μm and +30 μm TiB_2 particle-containing composites are shown in Figure 20. These photographs were obtained using a scanning elecron microscope. In general, the ceramic particles were observed to be substantially damage-free.

4.3.2 Friction and Wear Testing

All of the wear testing was performed on the in-house, CSDL-designed flex pivot wear tester that was described in the last annual report.[8] The testing was performed on the +30μm and -10μm specimens to see the effect of ceramic particle size on the wear and friction behavior of the material. The tests were conducted with sapphire, diamond, and TiB_2 composite pins contacting the selected 0.75-inch diameter, roughly 0.25 inch thick, disk composite specimen.

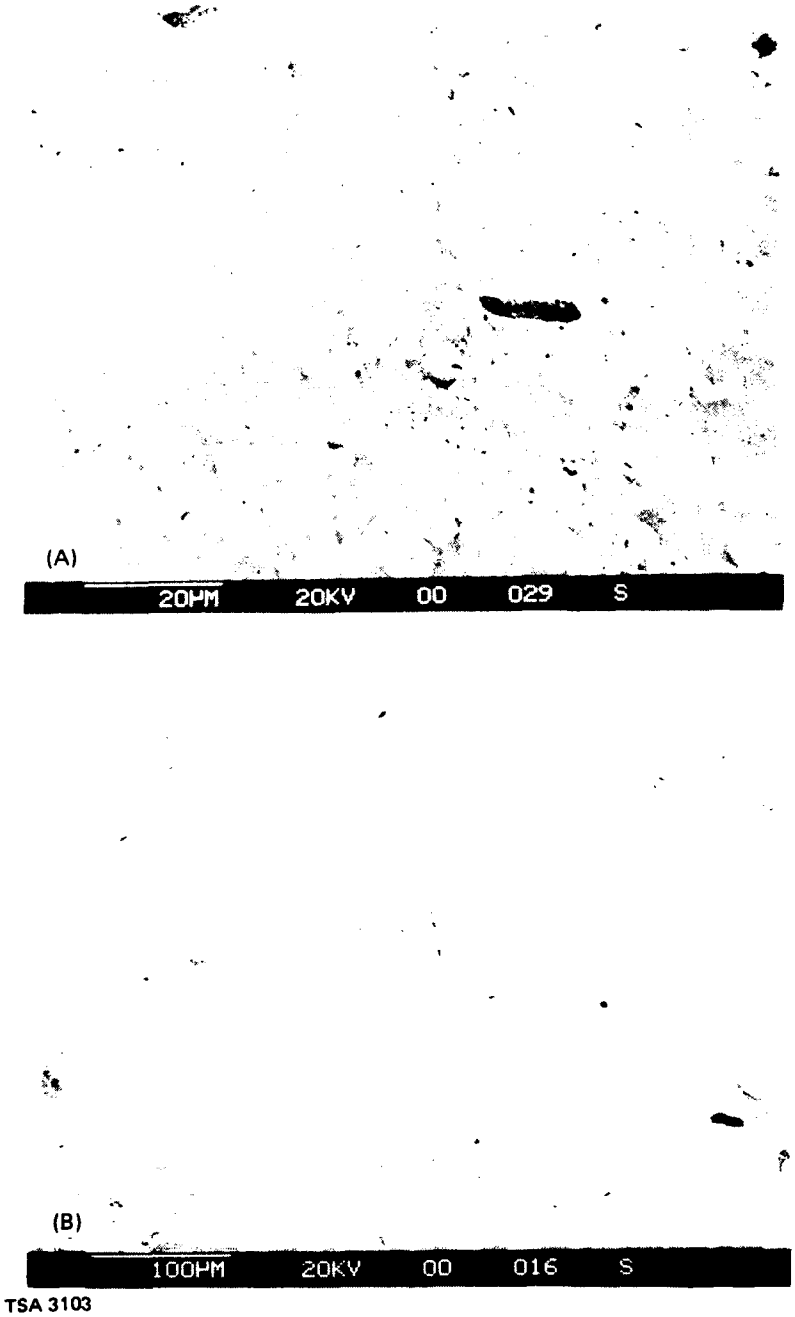

Figure 20. As HIP'ed microstructures of (A)-10μm and (B)+30μm TiB_2 composites. Different magnifications.

The composite disc was rotated at 100 r/min and friction traces obtained using a strip chart recorder. The values of the friction coefficients were calculated for these specimens at time intervals of 0.1, 1.0 and 10.0 minutes, which were measured from the start of the test. Friction traces were obtained at different applied loads. These were allowed to vary from 22 gms to about 300 gms. The results of these tests are shown in Table 10.

Table 10. Friction coefficient data on +30 and -10μm composite samples.

Run No.	Pin	Applied Load g	r/min	Friction Coefficient					
				+30μm TiB_2 (mins)			-10μm TiB_2 (mins)		
				0.1	1	10	0.1	1	10
1	Diamond	22	100	0.25	0.22	0.18	0.06	0.03	-
2	Diamond	30	100	0.12	0.11	0.07	0.14	0.11	0.08
3	Diamond	40	100	0.09	0.07	0.03	0.12	0.07	0.05
4	Diamond	5	100	0.09	0.07	0.05	0.57	0.49	0.34
5	Diamond	100	100	-	-	-	1.33	1.27	1.1
6	Diamond	150	100	0.12	0.08	0.07	0.21	0.08	0.08
7	Diamond	200	100	0.24	0.12	0.12	0.09	0.06	0.06
8	Diamond	300	100	0.06	0.06	0.06	-	-	-
9	Sapphire	20	100	0.17	0.59	0.92	0.14	0.64	1.01
10	-325 mesh	20	100	0.12	0.34	1.44	0.40	0.57	1.26

A substantial amount of scatter was observed in the data from these measurements. Data was collected for different applied loads to determine if a dependence of the friction coefficient on the applied load existed for the runs made with diamond pins that could be related to the wear phenomena in these composites in a manner similar to what was earlier observed for boron ion implanted specimens.[8] A further objective in the variation of the load was to determine if one of the two composites selected for evaluation was more susceptible to wear compared to the other. It was hoped that the more-susceptible-to-wear composite would show a more rapid evidence of wear in its friction traces (with increases in applied load) because of the influence of the wear debris generation process on the measured value of the friction coefficient. Values for the friction coefficients at different time, from the traces that were obtained, were, therefore, calculated with the hope that the variation in these values with time might also be indicative of a related wear process.

The measurements in Table 10 show that no appreciable dependence of either composite on applied load was achieved. Except for run numbers 1 and 7 for the +30μm composite and 4 and 5 for the -10μm composite, the data seemed fairly well behaved for wear runs versus a diamond stylus serving as the pin. The slight drop in the already low value of the friction coefficient with increasing time for most of the runs was interpreted as either resulting from the removal of an existing contaminating film on the surface or from a polishing action on rough surface irregularities that were initially present. In any event, the data showed that the two composites could not be differentiated for wear resistance potential using this procedure. In fact, both composites showed a superior wear resisting ability at loads which were much higher than would normally be encountered in an actual gas bearing. The data obtained with sapphire and composite pins resulted in substantially increased values of the friction coefficient which showed a significant rise with increasing time for both composites. This was expected for the sapphire pin on the basis of past observations on -325 mesh TiB_2-composite samples that had shown wear of the sapphire pins leading to a

build-up of wear debris on the composite surface. The present observations related to increased friction (and wear) with the composite pin would appear to indicate that these composite parts should not be allowed to mate with other similar composite parts in a wear circumstance such as what exists in a gas bearing.

Because the friction data proved insufficent for differentiating between the wear performing ability of the two composites, it was decided to examine the several wear tracks on the composites at high magnification using a scanning electron microscope. The observations in Figure 11 are typical of wear tracks observed using this technique on the two samples. The tracks appeared somewehat discontinuous in places as shown in Figure 21 even though at lower magnification these tracks appeared to be continuous. These observations, as other evaluations subsequently performed for changes in surface topography using a Dektak surface profilometer, were inconclusive with respect to the wear resisting ability of these materials.

4.3.3 Studies for Fabricating Parts of Acceptable Production Quality

Preliminary evaluations for the industrial use of this material were initiated through fabricating and testing of actual gas bearing hardware.[8] Several production related problems were encountered during this preliminary evaluation. The most notable among these were:

(1) development of appropriate lapping procedures for generating acceptable surfaces

(2) identification of suitable cleaning procedures following lapping

(3) machining of parts of cylindrical geometry with a hole running centrally about the axis from solid stock

(4) production of parts with a higher value of the thermal-expansion coefficient so it is more compatible with the beryllium structure.

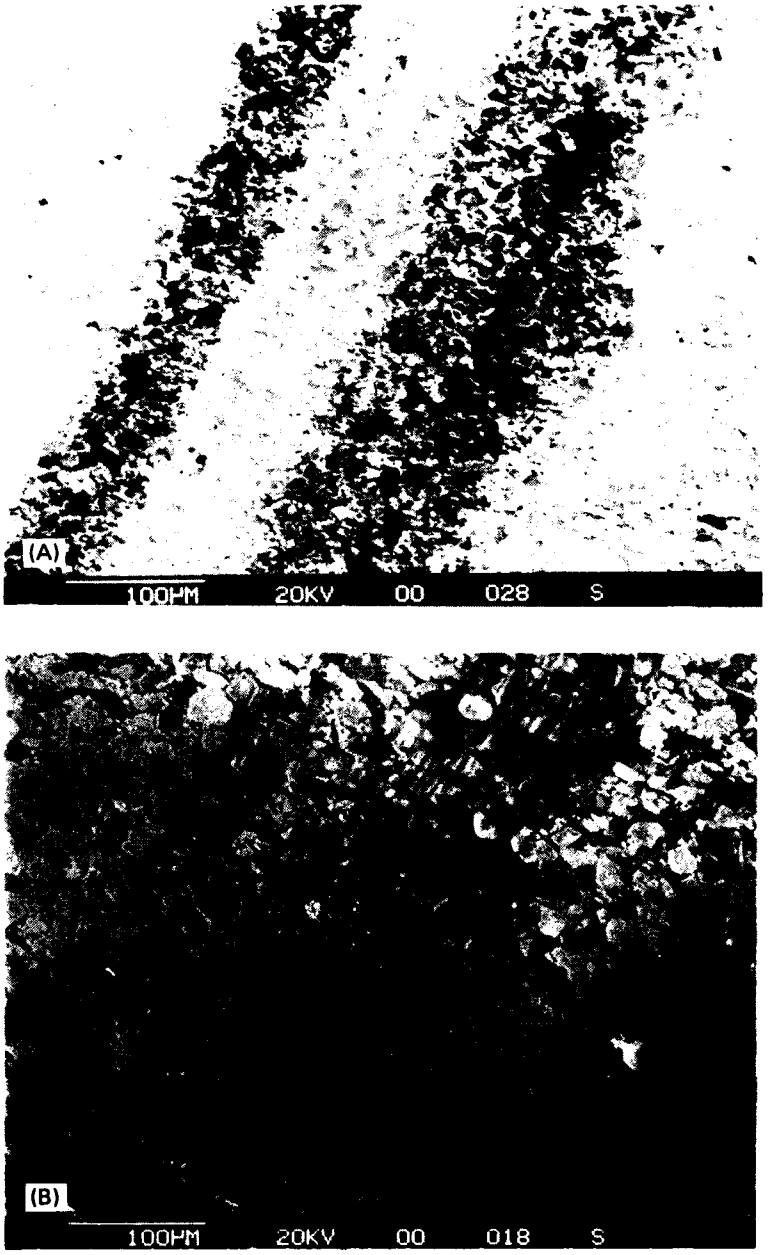

Figure 21. Wear tracks observed in (A)-10μm, (B)+30μm TiB_2 samples.

Even so, a few gas bearings were successfully assembled and have been demonstrated as good quality hardware that can perform well over a reasonable length of evaluation time.

The problems related to production of appropriately lapped surfaces were resolved along the lines described in an earlier section where good quality surfaces were obtained with minimum observable damage to the TiB_2 particles. Problems relating to suitable cleaning of the lapped parts were investigated and are described in 4.3.4. Also discussed are efforts made to produce near-net shape parts with the aim of minimizing machining concerns as well as increasing the thermal expansion coefficient of the fabricated parts to more closely match that of beryllium, which is the basic material for most of the structural components.

4.3.3.1 Effects of Ultrasonic Cleaning on Material Integrity

Observations made at the vendor's facility during the fabrication of the gas bearings indicated that continuous particulate generation resulted from an ultrasonic cleaning procedure that was used. Concerns raised in this regard included questions as to whether these parts could ever be cleaned thoroughly and whether continuous particulate generation was indicative of poor mechanical integrity of the material that might lead to catastrophic deterioration of the gas bearing during operation.

An initial, reasonably detailed examination, was, therefore, performed on an experimental part to confirm whether cleaning of the material using ultrasonic means results in degradation of the material. The experiments consisted of examination of a few selected areas on the as-received part. These were readily identifiable in that there were local areas of damage introduced during the earlier lapping process and subsequent examination of these same areas was performed each time after ultrasonic cleaning. The observations were made with a scanning electron microscope. The ultrasonic cleaner used was a Model SG-2 unit manufactured by the Blackstone Ultrasonics Company in Jamestown, New York. This unit was operated at the frequency designated by a setting of 100 on the dial. All of the cleaning was done in 80 ml of Freon inside a 150 ml laboratory beaker.

Observations typical of what was noted are shown in Figure 22. In Figure 22, the micrograph designated as (A) corresponds to the as-received condition, (B) the same region after 10 minutes of ultrasonic cleaning, and (C) the same region after an additional 20 minutes of cleaning (i.e., a total of thirty minutes in the ultrasonic cleaner). The micrographs indicated that in each instance, the minor changes that were noted had all occurred in the small pockets of damage that were present. The remainder of the material remained unchanged. These observations suggested that the composite parts should be cleaned as thoroughly as possible and fabrication procedures be developed that would minimize defect regions in the material. It was also suggested that substantially more care be exercised during the lapping process so as to drastically reduce, if not altogether eliminate, the occurrence of the pockets of damage that were observed.

Earlier efforts had shown that coarse TiB_2 particle sizes were probably more preferred for fabricating the composites because of an observed clustering of the fine (1-2 μm) TiB_2 particles in the grain boundary regions.[9]. These observations had, additionally, indicated that the coarse TiB_2 particles were more well bonded to the beryllium than were the finer particles. The foregoing had prompted the investigation into the fabrication of TiB_2-composites containing different sizes of ceramic particles. Ultrasonic experiments were, therefore, performed on composite samples belonging to the finest (-10μm) and the coarsest (+30μm) categories. These samples were lapped on their flat surfaces to a good finish using the refined lapping procedures, and the cylindrical surfaces were covered with an elastomeric film to minimize the cavitation-induced contribution to particulate generation from these rough surfaces. The experiments were not entirely successful in that the elastomeric film was observed to expand and separate away from the surface with each successive exposure to the ultrasonic environment. Particulate generation, in this instance, was monitored by light scattering from the particles which were suspended in the ultrasonic bath that consisted of PCA Freon.

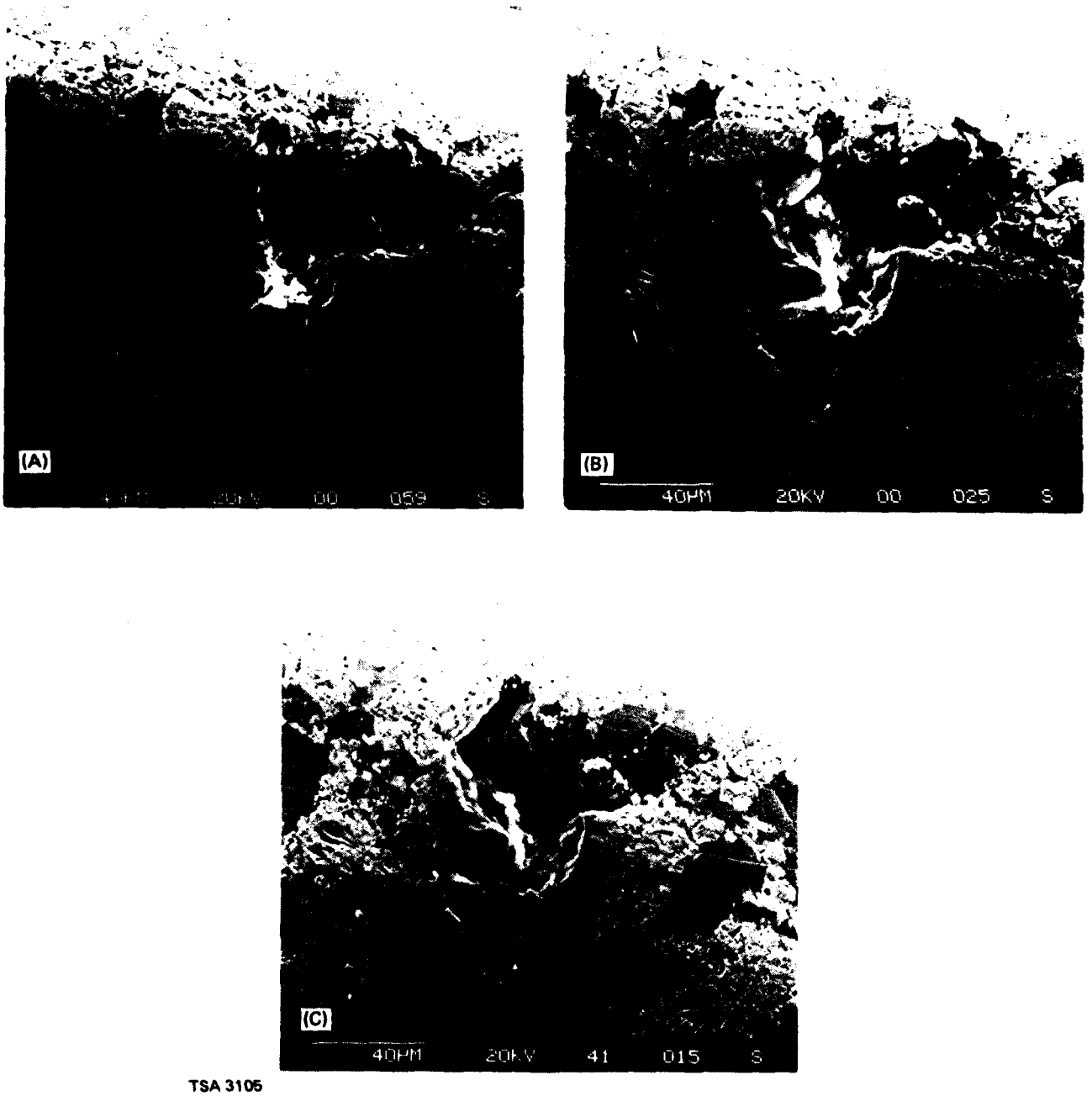

Figure 22. Region 1, low magnification. 2 large particles in (A) and (B) are removed in (C). No changes in surrounding areas.

(This liquid was filtered for particulates greater than 0.2μm prior to exposing the samples to this medium.) When ultrasonic cleaning was performed on these samples with a higher energy, Heat Systems, Inc. unit, it appeared that the -10μm composite produced more particles, as indicated by light scattering, than did the +30μm composite. In each case the amount of particulate generation was observed to decrease with each successive exposure. However, the amount of particulate production always remained at a finite level and was never observed to drop to a near-zero value. The particles were generally small but in some cases were as large as about 100μm. The particles were subsequently collected on a filter and examined using energy dispersive x-ray analysis on the SEM. It was surprising to find that only an extremely small minority of the particles were TiB_2. An equally small minority appeared to be beryllium (which could not be identified using this SEM/EDAX technique) Most of the other particles contained constituents such as Fe, Ti, and Si. Their origin cannot be explained. However, a tentative conclusion can, perhaps, be reached in that the effect of ultrasonic cleaning may not be as detrimental to composite integrity as was originally feared.

4.3.3.2 Near-Net Shape Fabrication of Gas-Bearing Parts

Work reported earlier had concentrated on the fabrication of solid composite parts shaped in the form of a cylinder with a hole running centrally along their axis. To minimize machining concerns, parts were produced using a central 430 stainless steel mandrel around which the composite material was HIPed. This stainless steel was selected on the basis of its close thermal expansion match to beryllium. However, even though single-point tool machining of the stainless was easier than that of the composite (which, however, can be ground with a fair degree of ease) machining was still quite difficult with the stainless and a decision was therefore made to use a low carbon steel as the inner mandrel in subsequent experiments.

Because of the dual objectives of minimizing, if not altogether eliminating, problems related to machining of the composite parts and of increasing the thermal expansion coefficient of the material to more

closely match that of beryllium, an alternative approach was selected. This consisted of fabricating the part essentially out of beryllium with no more than an 0.005 to 0.01 inch region of the surface consisting of the composition of the composite. This was expected to assure a high expansion coefficient (extremely close to beryllium) for the fabricated part as well as result in parts that could be produced with less severe machining constraints.

4.3.3.3 Beryllium Gas-Bearing Part Fabrication with Thin-Coating of Composite on Wear Surfaces

The part for the chosen gas bearing was an approximately 1/2-inch diameter beryllium cylinder, 1/2-inch high with a 1/4-inch hole at the axis of the cylinder. The two flat surfaces of the cylinder and the internal surface of the hole constituted the wear surface and therefore had to be protected with a low-friction wear-resistant coating such as that consisting of the TiB_2-composites. It was decided to put on such a coating by means of HIPing and for the first trial run the thickness of the coating was chosen to be roughly 0.010 inch.

Since HIPing would not significantly change the dimension of a solid piece of beryllium, a beryllium cylinder was machined such that the height was 0.020-inch smaller and the ID 0.025-inch larger than the desired finished dimensions. Under high pressure and at the elevated temperature used in the HIP technique sufficiently thick coatings of the composite were diffusion bonded to the flat surfaces as well as the internal diameter (ID) of the cylinder. The low carbon steel HIP cannister had a 1/16-inch wall and an ID which gave a snug fit to the beryllium cylinder. A 1/8-inch deep hole at the center of the flat 5/8-inch bottom of the HIP cannister allowed accurate positioning of a cylindrical mandrel concentric with the beryllium cylinder. The cylindrical mandrel of carbon steel was approximately 0.010-inch smaller than that of the finished rotor. Two special cylindrical tamping tools were machined, both of which were longer than the HIP cannister and had a hole drilled in the center to fit for free movement around the mandrel. The larger one had an OD to fit the ID of the HIP cannister,

and the smaller one fitted inside the ID of the beryllium cylinder. The fits were such that they provided free movement of the tamping tools. The loading of the HIP assembly was performed in the following manner.

The mandrel was first positioned in the cannister and a calculated amount of premixed composite powder (Be and TiB_2) was poured around the mandrel. The powder was leveled and packed densely using the large tamping tool. Next the beryllium cylinder was placed on the packed powder. The annular space between the beryllium and the mandrel was then fitted and tightly packed with the powder mixture using the smaller tamping tool. To assure a fill without voids, only small amounts of powder were used at a time and the process repeated many times until the space was completely filled with a high packing density. Next, another calculated amount of the powder was poured on top of the beryllium cylinder and tamped down with the larger tool. A 1/8-inch carbon steel disk of the same OD and ID as that of the beryllium cylinder was placed on top of the composite powder. The length of the mandrel was designed such that its top was nearly flush with the upper surface of the steel disk. Following the loading of the assembly, standard procedures were used to attach a proper pump out tube of cold rolled steel by welding. The assembly was subsequently evacuated, baked out, and the pump out tube pinched, following which it was HIPed at 1050°C for two hours under an Argon presure of 30 $lb/in.^2$.

REFERENCES

1. Keating, W.H., Compliance Coefficient Test Results for TGG No. 222X, Component Development Department, Memorandum No. 30H-76-541, The Charles Stark Draper Laboratory, Inc., December 1976.

2. Kumar, K., Analysis of $W_{(x)}C$ Sputter Deposits, Report No. C-4749, The Charles Stark Draper Laboratory, Inc., October 1976.

3. Markovsky, L. Ya, D. Kondraskev Yu, and G,V, Kaputovskaya, The Composition and Properties of Beryllium Borides, J. Gen. Chem. U.S.S.R., Vol. 25, 1955, p.1007.

4. Tupitsyn, I.I., I.I. Lyakhavskaya, M.S. Nakhamson, and A.S. Sukhik, Energy Structure of Beryllium Diboride, Sov. Phys. Sol. State, Vol. 16, No. 16, April 1975.

5. Hoenig, C.L., C.F. Cline, and D.E. Sands, Investigation of the System Beryllium-Boron, J. Am. Ceram. Soc., Vol. 44, No. 8, August 1961, p.385.

6. Laubengayer, A.W., D.T. Hurd, A.E. Newkirk, and J.L. Hoard, Preparation and Properties of Pure Crystalline Boron, J. Am. Chem. Soc., Vol. 65, 1943, p. 1924.

7. Croft, W.J., N.C. Tombs, and J.F. Fitzgerald, Preparation and Characterization of Boron Films from Diborane, Mat. Res. Bull., Vol. 5, 1970, p.489.

8. Das, D., K. Kumar, E. Wettstein, J. Wollam, Materials Research for Advanced Inertial Instruments, Task 2: Gas Bearing Material Development, Technical Report R-1528, The Charles Stark Draper Laboratory, Inc., December 1981.

9. Das, D., K. Kumar, E. Wettstein, J. Wollam, Materials Research for Advanced Inertial Instrumentation, Task 2: Gas Bearing Material Development, Technical Report R-1434, The Charles Stark Draper Laboratory, Inc., December 1980.

10. Kant, R., K. Kumar, A.R. Knudson, Mechanical and Microstructural Properties of Boron Implanted Beryllium, presented at the Mat. Res. Soc. 1981 Annual Meeting. Published in Proc. of Symp. E: Metastable Materials Formation by Ion Implantation; Editors: S.T. Piraux, W.T. Choyke, Elsevier Science Publishing Co., Inc., New York, 1982, p. 253.

11. Das, D., K. Kumar, Chemical Vapor Deposition of Boron on a Beryllium Surface, Thin Solid Films, Vol. 83, 1981, p. 53.

12. Ondracek, G., B. Leder, C. Politis, Quantitative Metallography of Metal-Ceramic Composites, Prakt. Metallogr., Vol. 5 (2), 1968, p. 71.

13. Rabinowicz, E. Friction and Wear of Materials, John Wiley and Sons, Inc., New York, 1965.

14. Kumar, K., D. Das, K. Koehler, Beryllium-Ceramic Composites Using HIP for Gas Bearings, 1981 Annual Meeting of the American Ceramic Society, Washington, DC.

15. Kumar, K., D. Das, Ceramic-Beryllium Composites for Gas Bearings, Am. Ceram. Soc. Bull., Vol. 62 (2), 1983, p. 249.

BASIC DISTRIBUTION LIST

Organization	Copies
Defense Documentation Center Cameron Station Alexandria, VA 22314	12
Office of Naval Research Department of the Navy 800 N. Quincy Street Arlington, VA 22217	
ATTN: Code 471	1
Code 102	1
Code 470	1
Commanding Officer Office of Naval Research Building 114, Section D 666 Summer Street Boston, MA 02210	1
Commanding Officer Office of Naval Research Branch Office 536 South Clark Street Chicago, IL 60605	1
Office of Naval Research San Francisco Area Office 760 Market Street, Room 447 San Francisco, CA 94102	1
Naval Research Laboratory Washington, DC 20375	
ATTN: Code 6000	1
Code 6100	1
Code 6300	1
Code 6400	1
Code 2627	1
Naval Air Propulsion Test Center Trenton, NJ 08628 ATTN: Library	1
Naval Construction Batallion Civil Engineering Laboratory Port Hueneme, CA 93043 ATTN: Materials Division	1
Naval Electronics Laboratory San Diego, CA 92152 ATTN: Electron Materials Science Division	1
Naval Missile Center Materials Consultant Code 3312-1 Point Mugu, CA 92041	1
Commanding Officer Naval Surface Weapons Center White Oak Laboratory Silver Spring, MD 20910 ATTN: Library	1
David W. Taylor Naval Ship Research and Development Center Materials Department Annapolis, MD 21402	1
Naval Undersea Center San Diego, CA 92132 ATTN: Library	1
Naval Underwater System Center Newport, RI 02840 ATTN: Library	1

BASIC DISTRIBUTION LIST (Continued)

Organization	Copies
Naval Air Development Center Code 302 Warminster, PA 18964 ATTN: Mr. F.S. Williams	1
Naval Air Systems Command Washington, DC 20360 ATTN: Codes 52031 52032	1
Naval Sea System Command Washington, DC 20362 ATTN: Code 035	1
Naval Facilities Engineering Command Alexandria, VA 22331 ATTN: Code 03	1
Scientific Advisor Commandant of the Marine Corps Washington, DC 20380 ATTN: Code AX	1
Naval Ship Engineering Center Department of the Navy Washington, DC 20360 ATTN: Code 6101	1
Army Research Office PO Box 12211 Triangle Park, NC 27709 ATTN: Metallurgy and Ceramics Program	1
Metals and Ceramics Division Oak Ridge National Laboratory PO Box X Oak Ridge, TN 37380	

Organization	Copies
Naval Weapons Center China Lake, CA 93555 ATTN: Library	1
Naval Postgraduate School Monterey, CA 93940 ATTN: Mechanical Engineering Department	1
NASA Headquarters Washington, DC 20546 ATTN: Code RRM	1
NASA (216) 433-400 Lewis Research Center 21000 Brookpark Road Cleveland, OH 44135 ATTN: Library	1
National Bureau of Standards Washington, DC 20234 ATTN: Metallurgy Division Inorganic Materials Division	1
Director Applied Physics Laboratory University of Washington 1013 Northeast Fortieth Street Seattle, WA 98105	1
Defense Metals and Ceramics Information Center Battelle Memorial Institute 505 King Avenue Columbus, OH 43201	1

BASIC DISTRIBUTION LIST (Continued)

Organization	Copies
Army Materials and Mechanics Research Center Watertown, MA 02172 ATTN: Research Programs Office	1
Air Force Office of Scientific Research Building 410 Bolling Air Force Base Washington, DC 20332 ATTN: Chemical Science Directorate	1
Electronics and Solid State Sciences Directorate	1
Air Force Materials Laboratory Wright-Patterson AFB Dayton, OH 45433	1
Library Building 50, Room 134 Lawrence Radiation Laboratory Berkeley, CA	1
Los Alamos Scientific Laboratory PO Box 1663 Los Alamos, NM 87544 ATTN: Report Librarian	1
Argonne National Laboratory Metallurgy Division PO Box 229 Lemont, IL 60439	1
Brookhaven National Laboratory Technical Information Division Upton, Long Island New York 11973 ATTN: Research Library	1
Office of Naval Research Branch Office 1030 East Green Street Pasadena, CA 91106	1

SUPPLEMENTARY DISTRIBUTION LIST

Organization	Copies
Jack Bouchard Northrop/PPD 100 Morse street Norwood, MA 02062	1
Howard Schulien Department 6209 Bendix Corporation Guidance Systems Divisions Teterboro, NJ 07608	1
Don Bates Honeywell, Inc. Aerospace Division 11350 US Highway 19 St. Petersburg, FL 33733	1
R. Baldwin Honeywell, Inc. Avionics Division 2600 Ridgway Parkway Minneapolis, MN 55413	1
Bus Brady 62-11B/1 Lockheed Missile and Space Co., Inc. PO Box 504 Sunnyvale, CA 94088	1
Dan Fromm MS 1A1 Delco Electronics 7929 South Howell Avenue Milwaukee, WI 53201	1
F. Mikoliet Autometics Division Rockwell International 3370 Miraloma Avenue Anaheim, CA 92803	1
P. Jacobson Sperry Flight Systems PO Box 21111 Phoenix, AZ	1
George R. Costello Senior Staff Engineer Control and Electromechanical Subdivision Guidance and Control Division The Aerospace Corporation PO Box 92957 El Segundo, CA 90009	1
John Hanks Dynamics Research Corporation 60 Concord Street Wilmington, MA 01887	1
D. Riley Systems Group, Minutemen TRW Inc. PO Box 1310 San Bernardino, CA 92402	1
Professor Robert Ogilvie Department of Materials Science and Engineering Massachusetts Institute of Technology Cambridge, MA 02139	
Dr. Glen R. Buell (D. Starks) AFML/MBT Wright-Patterson Air Force Base Dayton, OH 45433	1
Major George Raroha AFAL/CC Wright-Patterson Air Force Base Dayton, OH 45433	1

SUPPLEMENTARY DISTRIBUTION LIST (Continued)

Organization	Copies	Organization	Copies
Joe Jordan Litton Guidance and Control Systems 5500 Canoga Avenue Woodland Hills, CA 91364	1	Lt. Col. Gaylord Green Capt. Ken Wernle BMO/ENNG Norton Air Force Base San Bernardino, CA 92409	1
Bob Delaney Singer-Kearfott Division 150 Totowa Road Wayne, NJ 07470	1	Dave Gold (SP-230) Rick Wilson (SP-23411) Andy Weber (SP-23411) Strategic Systems Project Office Department of the Navy Washington, DC 20390	1
Elmer Whitcomb Sperry Gyroscope Division Great Neck, NY 11020	1	Lt. Col. Larry Fehrenbacker HQ/AFSC Andrews AFB, MD	1
C. Hoenig J. Holt R. Landingham Lawrence Livermore Laboratory University of California at Berkeley Livermore, CA 94550	1	N. Stuart (MMIRME) ALC/Ogden Ogden Air Logistics Command Hill AFB Ogden, UT 84404	1
Capt. S. Craig Aerospace Guidance Metrology Center Newark AF Station Newark, OH 43055	1	Professor R.M. Latanision Massachusetts Institute of Technology 77 Massachusetts Avenue Room E19-702 Cambridge, MA 02139	1
W. Lane Hamilton Standard Windsor Locks, CT	1	Dr. Jeff Perkins Naval Postgraduate School Monterey, CA 93940	1
Dr. A.G. Evans Department Material Sciences and Engineering University of California Berkeley, CA 94720	1	Dr. R.P. Wei Lehigh University Solid Mechanics Bethlehem, PA 18015	1
Professor H. Herman State University of New York Meterial Sciences Division Stony Brook, NY 11794	1	Professor H.G.F. Wilsdorf University of Virginia Department of Materials Science Charlottesville, VA 22903	

SUPPLEMENTARY DISTRIBUTION LIST (Continued)

Organization	Copies
Professor J.P. Hirth Ohio State University Metallurgical Engineering Columbus, OH 43210	1
Professor Peter Gielisse University of Rhode Island Division of Engineering Research Kingston, RI 02881	1
Dr. R.W. Rice Code 6360 Naval Research Laboratory 4555 Overlook Avenue, S.W. Washington, DC 20375	1
Professor G.S. Ansell Rensselaer Polytechnic Institute Department of Metallurgical Engineering Troy, NY 12181	
Professor J.B. Cohen Northwestern Univeresity Department of Materials Sciences Evanston, IL 60201	1
Professor M. Cohen Massachusetts Institute of Technology Department of Metallurgy Cambridge, MA 02139	
Professor J.W. Morris, Jr. University of California College of Engineering Berkeley, CA 94720	1
Larry Pope Sandia National Laboratories Division 5833 Alburquerque, NM 81785	1
Professor David Trunbull Harvard University Division of Engineering and Applied Physics Cambridge, MA 02139	1
Dr. D.P.H. Hasselman Montana Energy and MHD Research and Development Institute PO Box 3809 Butte, MT 59701	1
Dr. L. Hench University of Florida Ceramics Division Gainesville, FL 32601	1
Dr. J. Ritter University of Massachusetts Department of Mechanical Engineering Amherst, MA 02001	1
Professor G. Sines University of California at Los Angeles Los Angeles, CA 90024	
Director Materials Sciences Defense Advanced Research Projects Agency 1400 Wilson Boulevard Arlington, VA 22209	1

SUPPLEMENTARY DISTRIBUTION LIST (Continued)

Organization	Copies	Organization	Copies
Professor O.D. Sherby Stanford University Materials Sciences Division Stanford, CA 94300	1	Professor H. Conrad University of Kentucky Materials Department Lexington, KY 40506	1
Dr. E.A. Starke, Jr. Georgia Institute of Technology School of Chemical Engineering Atlanta, GA 30332	1		

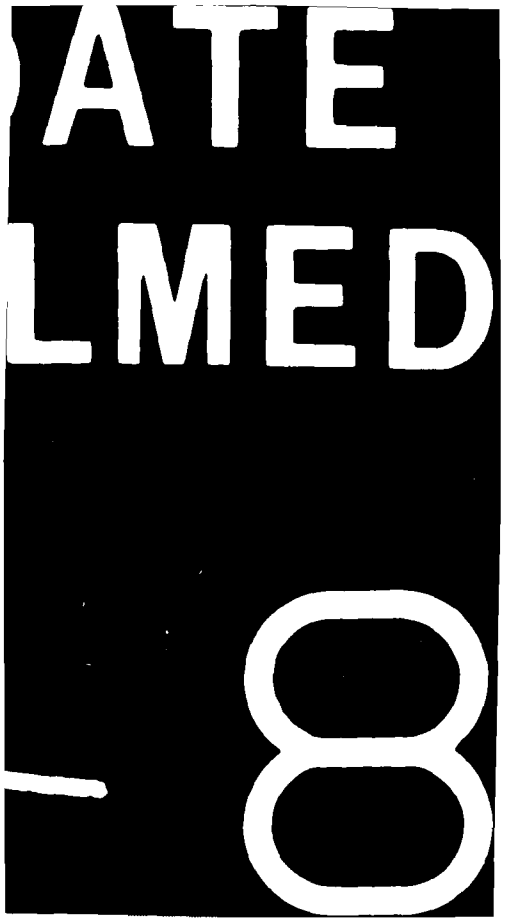
ATE
LMED
8